

# Critical Benchmarking of Popular Composite Thermochemistry Models and Density Functional Approximations on a Probabilistically Pruned Benchmark Dataset of Formation Enthalpies

Sambit Kumar Das,<sup>1</sup> Sabyasachi Chakraborty,<sup>1</sup> and Raghunathan Ramakrishnan<sup>1, a)</sup>  
*Tata Institute of Fundamental Research, Centre for Interdisciplinary Sciences, Hyderabad 500107, India*

(Dated: 23 May 2022)

First-principles calculation of the standard formation enthalpy,  $\Delta H_f^\circ$  (298 K), in such large scale as required by chemical space explorations, is amenable only with density functional approximations (DFAs) and some composite wave function theories (cWFTs). Alas, the accuracies of popular range-separated hybrid, ‘rung-4’ DFAs, and cWFTs that offer the best accuracy-vs.-cost trade-off have as yet been established only for datasets predominantly comprising small molecules, hence, their transferability to larger datasets remains vague. In this study, we present an extended benchmark dataset of over 1600 values of  $\Delta H_f^\circ$  for structurally and electronically diverse molecules. We apply quartile-ranking based on boundary-corrected kernel density estimation to filter outliers and arrive at Probabilistically Pruned Enthalpies of 1694 compounds (PPE1694). For this dataset, we rank the prediction accuracies of G4, G4(MP2), ccCA, CBS-QB3 and 23 popular DFAs using conventional and probabilistic error metrics. We discuss systematic prediction errors and highlight the role an empirical higher-level correction (HLC) plays in the G4(MP2) model. Furthermore, we comment on uncertainties associated with the reference empirical data for atoms and the systematic errors stemming from these that grow with the molecular size. We believe these findings to aid in identifying meaningful application domains for quantum thermochemical methods.

Keywords: thermochemistry, composite wave function theory, density functional theory, enthalpies of formation

## I. INTRODUCTION

An unmet promise in *ab-initio* quantum chemistry is to predict molecular and reaction enthalpies with such high an accuracy, that reaction energies and relative stabilities of constitutional/conformational/geometric isomers can be established in agreement with experimentally observed trends—but at a computational cost that is comparable to that of a density functional approximation (DFA) with a reasonably converged basis set<sup>1,2</sup>. This situation is apparent in the context of emerging data science campaigns, where computational explorations and statistical inference of molecular properties across *chemical compound space* is the prime focus<sup>3–8</sup>. Arguably, one of the most sought-after molecular properties for data-mining is the standard formation enthalpy,  $\Delta H_f^\circ$  (298 K), because of its significance to energetics and rates of industrial<sup>9,10</sup> and atmospheric chemical reactions<sup>11,12</sup>. Hence, development of a rapid thermochemistry protocol demonstrating a faithful transferability of accuracy from that of molecules used for the method’s benchmarking (*i.e. training*) to a query molecule—with arbitrary stoichiometry/valency and non-standard bond distances/angles—will remain an active research domain<sup>13–15</sup>.

Karton classified the most widely used composite

wavefunction theories (cWFTs) into those involving a post-CCSD(T)-level energy correction and those requiring a CCSD(T)-level treatment<sup>16</sup>. The former includes: W4<sup>17</sup>, HEAT-345QP<sup>18</sup>, and HEAT-456QP<sup>19</sup> which depend on higher-order terms in the coupled-cluster expansion (*i.e.* quadruple, quintuple and higher excitations) to forecast molecular energies of ‘high chemical accuracy’, with prediction error  $\leq 1$  kJ/mol<sup>20,21</sup>. Alas, the severe computational complexities of these methods restrict their applicability to small molecules with at most a few dozen electrons. The latter category of thermochemistry methods is dependent on electron correlation energy estimated only at the CCSD(T)-level, where the triples contribution is included perturbatively. Such a compromise extends the application domain of this class of methods—for instance, CBS-QB3<sup>22</sup>, G4<sup>23</sup>, ccCA<sup>24–26</sup> and their offshoots—to somewhat larger molecules with up to a couple of dozen main group atoms. Depending on the size of the basis set with which the CCSD(T) energy is estimated, cWFTs can yield an average prediction accuracy in the  $\approx 1 - 2$  kcal/mol range<sup>16</sup>. However, it must be noted that based on the computational complexity of these methods which scale unfavorably with molecular size, their application domain is restricted to molecules of size  $\text{CF}_4$  or  $\text{CH}_3\text{COOH}$  for FCI/CBS based methods,  $\text{C}_6\text{H}_6$  or  $\text{C}_6\text{H}_{14}$  for CCSDT(Q)/CBS based methods,  $\text{C}_{20}\text{H}_{20}$  for CCSD(T)/CBS methods, while CCSD(T)/TZ based methods can handle large systems like  $\text{C}_{60}$ .

A number of data-driven computational chemistry

<sup>a)</sup>Electronic mail: ramakrishnan@tifrh.res.in

benchmark studies have explored subsets of the GDB17 molecular universe<sup>27</sup> comprising 166,443,860,262 (*i.e.* 166.4 billion) closed-shell, organic molecules each containing up to 17 atoms of C, N, O, S, and halogens. These high-throughput computational studies have catered the data requirements of methodological studies focusing on machine learning (ML) modeling<sup>28,29</sup>. For instance, a past study has computed DFT-level structures and properties of a small subset of the GDB17 dataset with 133,885 small organic molecules (the QM9 dataset) each containing up to nine C, O, N and F atoms<sup>30,31</sup>. Recently, the QM9 dataset was subjected to rigorous G4(MP2) calculations reporting total energies, atomization energies and standard enthalpies of formation<sup>5,32</sup>. Other studies<sup>33,34</sup> have extended these works by applying ML and  $\Delta$ -ML<sup>31</sup> to statistically infer G4(MP2)-level energies of a small set of organic molecules containing more than 9 heavy atoms. On the basis of dataset size alone, these studies represent some of the massive high-throughput quantum chemistry efforts ever undertaken. However, it remains to be seen if these  $\Delta H_f^\circ$  values predicted with G4(MP2) for the QM9 dataset will be quantitatively accurate to a degree that is relevant for comparison with experiments.

The complexity involved in validating computed results in chemical space explorations is twofold: Firstly, it is a non-trivial task to automate the collection and pruning of available experimental energies for such a large dataset as QM9. Secondly, even if all these molecules are ‘synthetically feasible’, only a tiny fraction have been plausibly characterized by gas phase measurements. Seemingly, the only viable way of probing the transferability of a computational method to unexplored regions in the chemical space is to benchmark on compounds of similar chemical composition. In this context, Narayanan *et al.*<sup>5</sup> selected experimental values of  $\Delta H_f^\circ$  for 459 closed-shell hydrocarbons and their substituted analogues, containing atoms similar to those in the QM9 dataset, from Pedley’s extensive compilations<sup>35,36</sup> and observed an average prediction error of 0.8 kcal/mol for G4(MP2). This value is comparable to that of G4(MP2)’s<sup>37</sup> and ccCA’s<sup>38</sup> mean errors noted for similar molecules in the G3/05 small molecules dataset<sup>39</sup>. However, such high prediction accuracies are not expected to hold for electronically and structurally more diverse molecules that can be combinatorially generated from the QM9 set by protonation, deprotonation, or isovalence-electronic substitutions. For instance, Schwilk *et al.*<sup>40</sup> have selected about 4,000 molecules from the QM9 set and derived from this subset a new dataset QMspin, comprising 8000 triplet and 5000 singlet carbene compounds. To gain insight on the applicability of G4(MP2) to such non-trivial chemical subspaces, it is a timely pursuit to benchmark widely employed cWFTs on larger, curated benchmark datasets by extending upon existing thermochemistry benchmark sets.

In this study we aim to: (i) collect reference  $\Delta H_f^\circ$

values from several previous reports, include to these new benchmark datasets containing experimental results and present a consolidated dataset with  $\approx$  1.8k entries, (ii) apply a probabilistic procedure based on the best theoretical method applicable to the entire set to detect and eliminate potential outliers in the dataset, (iii) report on the prediction errors based on mean and percentiles metrics for the cWFTs, G4, G4(MP2), ccCA, and CBS-QB3 along with 23 popular DFAs and 2 semi-empirical methods, (iv) analyze the critical role of the HLC in the performance of G4(MP2) and comment on the method’s transferability, (v) from the larger dataset presented, identify and study a new benchmark set with isomerization reaction enthalpies for 32 sets of constitutional isomers, and (vi) finally, inspect the uncertainties in thermochemistry calculations arising due to the use of empirical reference data for atoms.

## II. COMPUTATIONAL DETAILS

G4(MP2), ccCA and DFAs-level thermochemistry calculations were automated through *in-house* scripts which rely on the ORCA suite of programs<sup>41,42</sup>. G4 and CBS-QB3 calculations were carried out with Gaussian suite of programs<sup>43</sup>. PM6<sup>44</sup> and PM7<sup>45</sup> calculations were done via the MOPAC suite of programs<sup>46</sup>. We considered 23 DFAs from various levels of Perdew’s ‘Jacob’s ladder’<sup>47</sup>, generalized gradient approximation (GGA): BLYP<sup>48</sup>, PW91<sup>49</sup> and PBE<sup>50</sup>; hybrid GGA: B3LYP<sup>51</sup>, O3LYP<sup>52</sup>, X3LYP<sup>53</sup> and PBE0<sup>54</sup>; meta-GGA: TPSS<sup>55</sup>; hybrid meta-GGA: TPSS0<sup>56</sup> and M06-2X<sup>57</sup>. We also selected the range-separated hybrid functionals: CAM-B3LYP<sup>58</sup>,  $\omega$ B97X<sup>59</sup>,  $\omega$ B97X-D3<sup>59</sup>,  $\omega$ B97X-V<sup>60</sup>,  $\omega$ B97M-V<sup>61</sup>,  $\omega$ B97X-D3BJ, and  $\omega$ B97M-D3BJ, where Grimme’s D3 dispersion with Becke-Johnson damping (D3BJ)<sup>62–65</sup> has been included explicitly. Furthermore, B2PLYP<sup>66</sup>, B2PLYP-D3<sup>67</sup> and mPW2PLYP-D<sup>68</sup> represent the double-hybrid functionals considered in this study, some of which include dispersion corrections. Additionally, we also benchmarked a few of the aforesaid functionals with an additional dispersion correction, namely, B3LYP-D3, TPSS0-D3 and M06-2X-D3.

Initial geometries for molecules from previously studied datasets were collected from their corresponding sources—when such information was available—and subjected to geometry relaxations. For compounds with no previously reported geometries, we consulted the popular online chemical databases: NIST<sup>69</sup>, ChemSpider<sup>70</sup> and Pub-Chem<sup>71</sup>. In some cases, we created initial geometries using the software Avogadro<sup>72</sup> and performed minimum energy geometry relaxation with universal forcefield (UFF)<sup>73</sup>. We performed all DFA calculations at the B3LYP/6-31G(2df,p) minimum energy geometry in a single point fashion using the def2-QZVP basis set, that has been shown to yield predictions close to the Kohn-Sham limit<sup>74</sup>. PM6 and PM7

calculations were performed using precise geometry relaxation thresholds at the corresponding levels. Geometry optimizations with DFAs were carried out with tight convergence criteria with  $10^{-4}$  as the threshold for the maximum component of the force vector. To facilitate convergence of the geometry towards the energy minimum, force constants were computed at every fifth step of geometry optimization. In all calculations, SCF convergence was reached with `verytightscf` criteria corresponding to a threshold of  $10^{-9}$  Hartree for the electronic energy. For the numerical quadrature of the exchange correlation part of the energy in DFAs, we used Lebedev-434 angular grids and Grid7 settings for Gauss-Chebyshev radial grids. From the zero-point corrected electronic energy,  $\Delta H_f^\circ$  (298K) was calculated according to the standard convention<sup>75</sup>. Heats of formation of atoms at 0 K,  $\Delta H_f^\circ(0\text{ K})$ , and enthalpy corrections, for elements in their standard states,  $H^\circ(298\text{ K}) - H^\circ(0\text{ K})$  are listed in APPENDIX. Spin-orbit corrections to the electronic energies of atoms, ions, selected diatomic molecules<sup>76</sup> and acetylene were collected from Refs. 23, 77, and 78.

### III. COMPOSITE WAVEFUNCTION THEORIES: G4(MP2) AND CCCA

cWFTs provide molecular thermochemical properties by exploiting the transferability of hierarchical corrections to electronic energies and thermal contributions. In Fig. 1, we present the famous Pople diagram where the desired, albeit expensive, target (non-relativistic) electronic energy at the CCSD(T)/CBS-level can be reached via 3 equivalent additivity routes that is encoded in the G4(MP2) method:

I Reference energy at CCSD(T)/S (small basis) with basis set corrections for electron correlation energy at MP2/S $\rightarrow$ L (small to large basis), and basis set correction for SCF energy HF/L $\rightarrow$ CBS (large to complete basis set).

II Reference energy at MP2/L with post-MP2 correlation with MP2 $\rightarrow$ CCSD(T)/S and basis set correction for SCF energy with HF/L $\rightarrow$ CBS corrections, or

III Reference energy at HF/CBS with electron correlation energy estimated jointly at HF $\rightarrow$ MP2/L and MP2 $\rightarrow$ CCSD(T)/S levels.

The ccCA method differs from G4(MP2) by exactly capturing the MP2-level correlation contribution through a CBS extrapolation of the MP2 energy, and includes post-MP2 level correlation correction with the CCSD(T) method using a triple-zeta basis set. ccCA has separate terms for the relativistic correction and the core-valence effect while G4(MP2) relies on an empirical term – higher level correction (HLC). Both methods account for zero-point vibration energy (ZPVE) by scaling the

harmonic frequencies along with atomic and diatomic spin-orbit (SO) corrections.

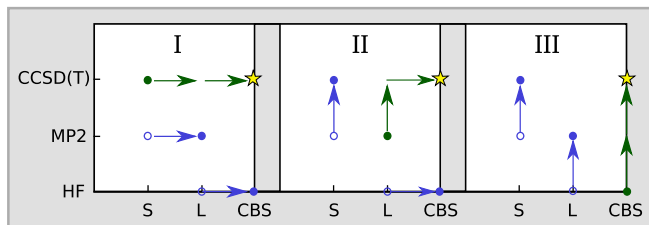


FIG. 1. Three paths to approximate chemical accuracy. Green circle refers to a baseline energy. Green arrows point to exact corrections, while blue arrows correspond to approximate corrections. Blue solid circles imply energy evaluated with a separate calculation while blue open circles imply energy available without an additional calculation. In I, CCSD(T)/S is the starting point while MP2/L, and HF/CBS are the starting points in II and III.

G4(MP2)<sup>37</sup> uses a minimum energy geometry at the B3LYP/6-31G(2df,p)-level (basis set henceforth referred to as GTBAS3), followed by a single-point energy calculation at the CCSD(T)/6-31G(d)-level (basis set henceforth referred to as GTBAS1). For molecular enthalpies, vibrational wavenumbers and ZPVEs are calculated using B3LYP/GTBAS3 with harmonic wavenumbers scaled by 0.9854 to approximately account for the missing anharmonic effects<sup>75</sup>. Basis set corrections are included through single point energy corrections at MP2 and HF levels through a focal-point analysis<sup>79</sup> (see Fig. 1). *Gn*-series closely follows Route-I in Fig. 1, where the expensive  $E_{\text{CBS}}^{\text{CCSD(T)}}$  target is estimated as

$$E_{\text{CBS}}^{\text{CCSD(T)}} \approx E_{\text{GTBAS1}}^{\text{CCSD(T)}} + \Delta E^{\text{MP2}} + \Delta E^{\text{HF}} \quad (1)$$

$\Delta E^{\text{MP2}}$  providing the basis set effect on the correlation energy and  $\Delta E^{\text{HF}}$  aiming to improve the HF energy to the HF-limit:

$$\Delta E^{\text{MP2}} = E_{\text{G3MP2LargeXP}}^{\text{MP2}} - E_{\text{GTBAS1}}^{\text{MP2}} \quad (2)$$

G3MP2LargeXP is a modified form of the 6-311+G(3df,2p) basis set with 3df polarization functions for the first row elements, 4d2f functions for the second row elements and 3d2f functions for the third row elements.

$$\Delta E^{\text{HF}} = E_{\text{CBS}}^{\text{HF}} - E_{\text{G3MP2LargeXP}}^{\text{HF}}, \quad (3)$$

where the HF-limit energy,  $E_{\text{CBS}}^{\text{HF}}$ , is obtained through a two-point extrapolation of HF/mTZ and HF/mQZ energies:

$$E_{\text{CBS}}^{\text{HF}} = (E_{\text{mQZ}}^{\text{HF}} - e^{-\alpha} E_{\text{mTZ}}^{\text{HF}}) / (1 - e^{-\alpha}) \quad (4)$$

where  $e$  is the base of the natural logarithm, and  $\alpha = 1.63$ . The mXZ basis sets are modifications of the corresponding aug-cc-pVXZ basis sets with an inclusion

of tight  $d$  function for the atoms Al-Ar. To reduce the computational cost, the number of diffuse functions on heavy atoms and the size of the hydrogen basis set are trimmed. For detailed descriptions regarding modifications to all the basis sets, please see Refs. 23, 37, 78, and 80.

The total G4(MP2) electronic energy takes the form

$$E_0^{\text{G4(MP2)}} = E_{\text{GTBAS1}}^{\text{CCSD(T)}} + \Delta E^{\text{MP2}} + \Delta E^{\text{HF}} + \text{ZPVE} + \text{SO} + \text{HLC} \quad (5)$$

The HLC term, as pointed out by Martin<sup>21,81-84</sup>, accounts for the residual error introduced in the additive model when there is significant coupling between the one-particle basis set and  $N$ -electron correlated wavefunction. However, it is long known that the success of the HLC correction in  $G_n$  methods is strongly coupled to the choice of basis sets employed. To quote John Pople<sup>85</sup>—from the first study on the G1 method—“Uniform application of the HLC is only sensible if the basis used, 6-311+G\*\*(2df), is reasonably balanced, meaning that residual errors per electron are approximately constant over a wide range of molecules.”. HLC has been modified over the years through G1<sup>85</sup>, G2<sup>86</sup>, G3<sup>80</sup> and G4<sup>23</sup> studies. In G4(MP2)<sup>37</sup>, the HLC terms take the same form as in G4 but with parameters optimized separately:

$$\text{HLC}^{\text{G4(MP2)}} = \begin{cases} -An_\beta \\ -A'n_\beta - B(n_\alpha - n_\beta) \\ -Cn_\beta - D(n_\alpha - n_\beta) \\ -E \end{cases} \quad (6)$$

where the terms bear the same meaning as in the original G4 study<sup>23</sup>.

On the other hand, the ccCA method, developed by Wilson *et al.* is devoid of any such empirical term<sup>24</sup>. As in the G4(MP2) method, ccCA depends on a reference geometry and harmonic vibrational frequencies computed with B3LYP/GTBAS3. The baseline for ccCA is the MP2-limit energy,  $E_{\text{CBS}}^{\text{MP2}}$ , with correlation energy corrections,  $\Delta E^{\text{CC}}$ , included at the CCSD(T)/cc-pVTZ level. Of the many ccCA variants developed by Wilson *et al.*<sup>24,25,38,87-89</sup>, here, we consider ccCA-P<sup>25</sup>, henceforth referred as ccCA. This method uses a 3-point extrapolation formula to determine  $E_{\text{CBS}}^{\text{MP2}}$ ,

$$E(x) = E_{\text{CBS}} + Be^{-(x-1)} + Ce^{-(x-1)^2}, \quad (7)$$

where  $x = 2, 3$  and 4 correspond to MP2/aug-cc-pVXZ ( $X = \text{T, D, and Q}$ ) energies, respectively, and gets simplified to:

$$E_{\text{CBS}}^{\text{MP2}} = (\alpha_1 E_{\text{DZ}}^{\text{MP2}} - \alpha_2 E_{\text{TZ}}^{\text{MP2}} + \alpha_3 E_{\text{QZ}}^{\text{MP2}}) / \beta \quad (8)$$

where,  $\alpha_1 = 1 + e^2$ ,  $\alpha_2 = e^1 + e^3 + e^5$ ,  $\alpha_3 = e^6$ , and  $\beta = (e - 1)(e^5 - e^2 - 1)$ . The final working equation for ccCA stands as

$$E_0^{\text{ccCA}} = E_{\text{CBS}}^{\text{MP2}} + \Delta E^{\text{CC}} + \Delta E^{\text{DK}} + \Delta E^{\text{CV}} + \text{ZPVE} + \text{SO} \quad (9)$$

where  $\Delta E^{\text{DK}}$  accounts for scalar relativistic correction calculated using the spin-free, one-electron Douglas-Kroll-Hess Hamiltonian of second-order (DKH2)<sup>90-93</sup> with frozen-core MP2 energy at cc-pVTZ-DK basis sets, whereas  $\Delta E^{\text{CV}}$  accounts for core-valence correlation effects (see Refs. 24, 25, and 94).

ZPVE & SO are the zero-point vibration energy (computed with a scaling factor of 0.9854<sup>75</sup>) and spin-orbit correction terms, respectively. For the first-row atoms, the MP2 calculation accounts for correlation effects from all electrons, while for the second- and third-row atoms, only those electrons in the  $K$ -shell, and  $K, \&L$ -shells are kept frozen, respectively. Further, ccCA employs tight- $d$  basis sets—cc-pV( $x + d$ )Z, aug-cc-pV( $x + d$ )Z and aug-cc-pCV( $x + d$ )Z—for second-row elements (Na-Ar) to consider core polarization effects and core-valence basis sets for Ga-Kr developed by Wilson *et al.*<sup>95,96</sup>.

#### IV. BENCHMARK DATASET OF MOLECULAR STANDARD FORMATION ENTHALPIES

We have gathered benchmark values of  $\Delta H_f^\circ$  from six previously studied datasets amounting to 2,204 entries:

1. G3/05 dataset<sup>39</sup> is a set of 454 energies distributed into: 270  $\Delta H_f^\circ$ , 105 ionization energies (IE), 63 electron affinities (EA), 10 proton affinities (PA), and 6 binding energies (BE) of hydrogen-bonded complexes. This set has been extensively used in the development of the  $G_n$  theories and also in the validation of other *ab initio* thermochemical protocols. We have selected 247 values of  $\Delta H_f^\circ$  from this set. We note in passing that the original dataset included 23 atomization energies which we exclude here.
2. Alexandria dataset<sup>97</sup> contains classes of molecules similar to that of G3/05 but larger in number with variations in molecular size, thus, providing a platform to examine the transferability of methods that perform well for G3/05. Out of 2704 entries in this dataset, 1383 compounds that contain experimental values of  $\Delta H_f^\circ$  have been selected.
3. Pedley CHONF is a set derived from 459 experimental values for hydrocarbons and substituted hydrocarbons from Pedley’s report<sup>36</sup> containing the atoms H, C, N, O, and F. An earlier study<sup>5</sup> benchmarked the accuracy of G4(MP2) for this dataset and reported an average prediction error of 0.8 kcal/mol.
4. ISO-8 comprises experimental isomerization energies—derived from  $\Delta H_f^\circ$ —for 8 sets of constitutional isomers amounting to 64 entries<sup>98</sup>.

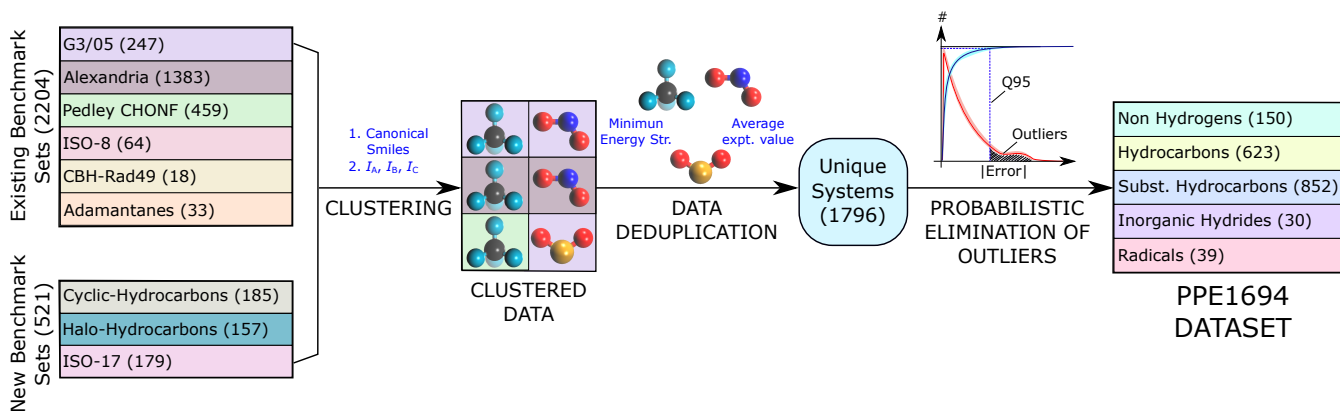


FIG. 2. PPE1694 dataset of molecular standard formation enthalpies: Data collection, deduplication and probabilistic filtering of outliers. See text for more details of the individual datasets and their sources.

- From Sengupta *et al.*<sup>99</sup> containing a collection of 49 cyclic & acyclic radicals with diverse functional groups with reference  $\Delta H_f^\circ$  energies gathered from experiment and high-level theoretical modeling, we collect only 18 entries in CBH-Rad49 with experimental references.
- Adamantanes comprises Dorofeeva *et al.*'s<sup>100</sup> dataset of 33 adamantanes for which  $\Delta H_f^\circ$  were estimated by simultaneous least-squares regression of a thermochemical network containing 300 isodesmic reactions.

Among all the datasets considered here, only G3/05 has been studied with DFT, WFTs and cWFTs<sup>37–39</sup>, hence, serve as a critical dataset to evaluate the accuracy of thermochemistry methods. To further enrich the benchmark set, we included 521 compounds from Refs. 35 and 36 that have never been subjected to theoretical modeling; these compounds belong to the following three categories: cyclic hydrocarbons, halogen-rich hydrocarbons and constitutional isomers with 17 unique stoichiometries (ISO-17). The number of compounds added from each of the aforesaid dataset is shown in Fig. 2. The total number of compounds from the collective set amounts to 2725, where we found a number of repeated entries. To eliminate redundant values, we followed a systematic data deduplication procedure which compares molecular stoichiometries, principal moments of inertia of the geometry and heavy atom bond counting. Firstly, we separated the radicals and non-radicals and binned them appropriately based on their stoichiometries. Following this, we investigated the canonical smiles, principal moment of inertia of every molecule which shared a particular stoichiometry and clustered those with similar canonical smiles and(or) principal moment of inertia. Finally, from this clustered set the average experimental value was considered and the conformer with the least theoretical value from G4(MP2) value were chosen.

Following de-duplication, 2725 entries reduced to 1796 unique entries, for which it is a non-trivial task to quantify—*ab initio*—plausible uncertainties arising not only from random and systematic errors in the experimental measurements, but also due to ambiguities associated with the empirical parameters used in the estimation of  $\Delta H_f^\circ$ . Paulechka *et al.*<sup>101</sup> have discussed the reasons for typical uncertainties in experimentally determined  $\Delta H_f^\circ$  and indicated that these could be of the order of even a few kJ/mol. In that study, for very critical benchmarking of the DLPNO-CCSD(T) based estimation of  $\Delta H_f^\circ$ , the authors have selected 45 compounds for which at least two independent experimental results were available. Even when using such ‘precise’ experimental values as references, error trends based on the mean unsigned error (MUE) can severely underestimate thermochemical uncertainty<sup>102</sup>. Simm *et al.*<sup>103</sup> have discussed how a performance analysis based on MUE is prone to fail as it does not distinguish the systematic contributions to the errors from the non-systematic counterparts. For pathological error distributions, arising plausibly due to the presence of outliers in the reference dataset, prediction uncertainties can be truncated using percentile-based error metrics<sup>102,104–106</sup>. More specifically, performance ranking of *ab initio* methods revealing trends in uncertainties has been made possible by the use of the 95<sup>th</sup> percentile of the absolute intensive (*i.e.* normalized) error distributions along with the MUE<sup>107</sup>. It is the subject of Section V to discuss a procedure to detect probabilistic tendencies of a reference datum from the 1796 set to be an outlier.

## V. PROBABILISTIC PRUNING OF THE DATASET

Following the data deduplication step, we utilize a probabilistic argument to detect outliers in the resulting dataset with 1796 entries. The basic principle behind this scheme is to utilize highly accurate computed val-

ues of  $\Delta H_f^\circ$  as references and mark only those molecules that lie beyond the 95<sup>th</sup> percentile of the error distribution as outliers. The cumulative probability used for this purpose acts as a prior distribution—more robust the reference method, more reliable the prior probability is. Hence, it may be anticipated that this scheme is guaranteed to detect genuine outliers when one of the high-precision methods such as W4, HEAT-456QP, or HEAT-345QP is used as a reference. Given the size of majority of the molecules in the dataset, we depend on G4 predicted values to define the prior probability. Owing to high computational cost for 20 systems in the 1796 set, we relied on G4(MP2) values instead of G4 values. Further computational details of the calculations performed are deferred to Section III

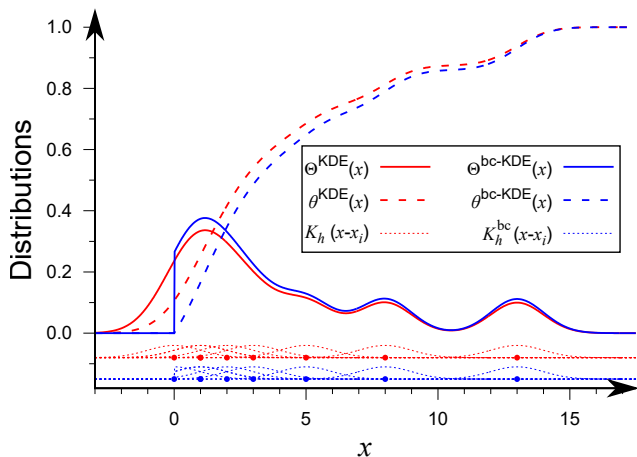


FIG. 3. Probability density function,  $\theta(x)$ , and cumulative distribution function,  $\Theta(x)$ , based on kernel density estimation (KDE) and its boundary corrected analog, bc-KDE, demonstrated for an exemplary dataset with eight points:  $x_1 = 0$ ,  $x_2 = x_3 = 1$ ,  $x_4 = 2$ ,  $x_5 = 3$ ,  $x_6 = 5$ ,  $x_7 = 8$  and  $x_8 = 13$ . For clarity,  $\theta(x)$  has been multiplied by 100. Also shown in the bottom of the plot are the kernel basis functions  $K_h(x - x_i)$  and  $K_h^{\text{bc}}(x - x_i)$  centered at the data points with arbitrarily shifted ordinates.

We begin with the absolute errors in the G4 predicted  $\Delta H_f^\circ$  for the 1796 set. We followed the arguments presented by Savin *et al.*<sup>108</sup> and Perdew *et al.*<sup>109</sup>, and chose an intensive error measure in order to account for the fact that the dataset contains molecules covering various sizes. For this purpose, we used MUE per valence electron, to capture periodic trends in molecular thermochemistry. From the discrete values of the G4 error, we obtain a continuous probability distribution using the boundary corrected kernel density estimation (bc-KDE), where a radial basis function is expanded at each discrete value of the error. In KDE, we take a kernel in the form of the standard normal distribution  $\mathcal{N}(0, 1)$

$$K_h(x - x_i) = \frac{1}{\sqrt{2\pi}h} \exp\left[-\frac{(x - x_i)^2}{2h^2}\right], \quad (10)$$

where  $K_h$  is the normalized estimator. A kernel function is expanded at every data point, giving rise to the (un-normalized) total density function that is an average of all kernels

$$\hat{f}(x, h) = \frac{1}{N} \sum_{i=1}^N K_h(x - x_i) \quad (11)$$

It is a well-known problem that KDE can delocalize beyond the allowed domain; in such cases, the naive approach of truncating the total density function  $f(x)$  often underestimates the actual probability distribution. This effect is illustrated using a toy dataset in Fig. 3. To this end, we employ boundary-corrected kernels of the form

$$K_h^{\text{bc}}(x - x_i) = [K_h(x - x_i) + K_h(x + x_i - 2x^*)] \mathbf{1}_{x \in A}, \quad (12)$$

where the indicator function  $\mathbf{1}_{x \in A}$  is 1 when  $x \in A$  and vanishes otherwise<sup>110</sup>. As is evident from Fig. 3, the bc-KDE captures the true nature of the probability density when the property is bounded. While the individual kernel functions that cross the boundary are truncated by the indicator function, the total probability is still conserved through a normalization of the resulting probability density, see Eq. 14.

In our bc-KDE calculations, we used a kernel width of 0.005 kcal/mol and determined the total density function as the average

$$\hat{f}(x, h) = \frac{1}{N} \sum_{i=1}^N [K_h(x - x_i) + K_h(x + x_i - 2x^*)] \mathbf{1}_{x \in A}, \quad (13)$$

which is normalized over the domain to give the probability density function (PDF)

$$\hat{\phi}(x) = \frac{\hat{f}(x, h)}{\|\hat{f}(x, h)\|_2}. \quad (14)$$

The cumulative density function (CDF) used to identify percentiles is obtained by integrating the PDF

$$\hat{\Phi}(x) = \int_A^B dx \hat{\phi}(x). \quad (15)$$

The resulting CDF enables statistical modeling of the probability to obtain a certain degree of prediction accuracy for a given quantum chemistry method as previously noted by Pernot *et al.*<sup>104</sup>. To estimate the variance of the CDF, we followed bootstrapping with 1000 shuffles, with 500 points randomly sampled from the 1796 set. The boundary-corrected kernel density probability distribution,  $\theta^{\text{bc-KDE}}$  and the corresponding cumulative density function  $\Theta^{\text{bc-KDE}}$  are on display in Fig. 4. To eliminate any sampling bias, we use the lower bound of the 95<sup>th</sup> percentile, denoted  $Q_{95}^-$  in Fig. 4 as

a threshold; all compounds for which the MUE per valence electron is greater than  $Q95^-$  are marked as outliers and eliminated from the dataset. We thus arrive at the benchmark set of probabilistically pruned enthalpies of 1694 compounds, denoted henceforth PPE1694. In this way, elimination of 102 outliers from the original 1796 set, decreased G4(MP2)'s MUE for the dataset from 2.17 kcal/mol to 1.70 kcal/mol. This final MUE is 0.71 kcal/mol larger than the methods MUE for the G3/05 dataset with 270 values of  $\Delta H_f^\circ$ . In Section VID, we discuss how the performance of cWFTs and DFAs deteriorate systematically because of the uncertainties associated with empirical atomic parameters used in the calculation of thermochemistry energetics. Compared to the small molecules benchmark set G3/05, PPE1694 covers the space of molecules that contain more atoms as well as more valence electrons; qualitative trends are illustrated in Fig. 5. The largest number of valence electrons in G3/05 and PPE1694 sets are 66 ( $C_6F_6$  and  $C_6F_5Cl$ ) and 166 ( $C_{10}F_{18}$ ), respectively. On the other hand, the maximum number of atoms in a given compound is 26 ( $C_8H_{18}$ ) for the G3/05 set, and 56 ( $C_{18}H_{37}Cl$ ) for PPE1694. Both sets are dominated by closed-shell molecules as evident from larger counts for compounds with even number of valence electrons, see Fig. 5a.

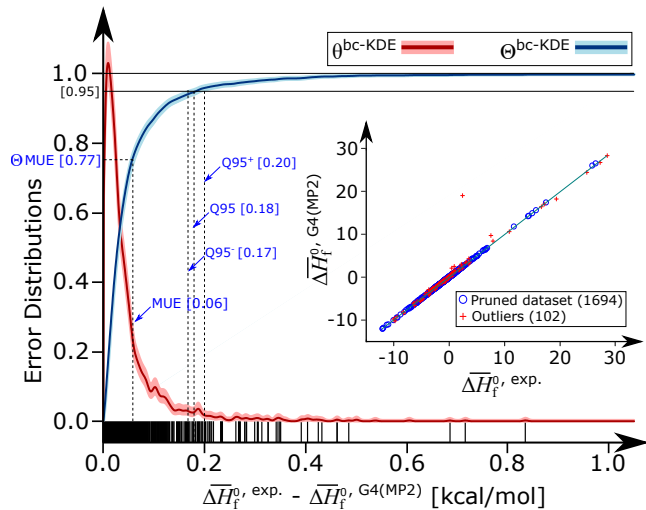


FIG. 4. Boundary-corrected kernel density probability distribution,  $\theta^{bc-KDE}$  and the corresponding cumulative density function  $\Theta^{bc-KDE}$  for the absolute deviations of G4(MP2)-predicted  $\Delta H_f^\circ$  from the experimental ones for 1694 compounds. The overline indicates that the values are normalized over valence electrons. Uncertainty envelopes were determined by bootstrapping. The inset features a scatterplot.

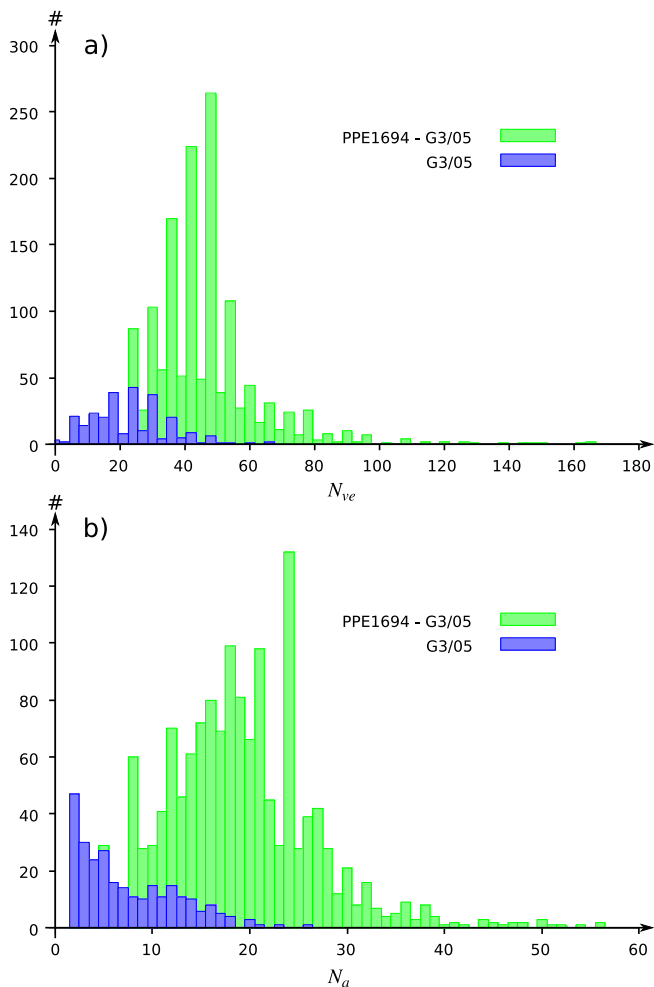


FIG. 5. Distribution of compounds in the G3/05 dataset compared to other molecules that are present in PPE1694: a) Counts for number of valence electrons  $N_{ve}$ , b) Counts for number of atoms  $N_a$ .

## VI. RESULTS AND DISCUSSIONS

### A. Benchmark results for cWFTs and DFAs

While cWFTs are the recommended choice for modeling  $\Delta H_f^\circ$ , the favorable accuracy-to-speed trade-offs of DFAs have facilitated  $\Delta H_f^\circ$  predictions for large molecules through isodesmic reaction schemes<sup>111,112</sup> and group additivity schemes<sup>113</sup>. A benchmark across popular DFAs on a curated dataset such as PPE1694 (see Fig. 5), may provide insights into how the performances of these methods can be refined through proper selection of basis sets and additional dispersion corrections. To this end, we embark upon comprehensive benchmarking of G4, G4(MP2), ccCA, CBS-QB3, 23 popular DFAs as well as the semi-empirical methods, PM6 and PM7.

Table I summarizes MUEs, RMSEs and maximum

TABLE I. Prediction errors in the modeling of  $\Delta H_f^\circ$ . For selected cWFTs, DFAs and semi-empirical methods, mean unsigned error (MUE) is reported for each class of compounds in the PPE1694 benchmark dataset. The root-mean-square-error is given in parenthesis while, the most positive and negative errors are provided inside a square bracket. All values are in kcal/mol.

Methods	Nonhydrogens (150)	Hydrocarbons (623)	Subst. hydrocarbons (852)	Inorganic hydrides (30)	Radicals (39)	Total (1694)
G4(MP2)	2.21 (3.31) [-12.33, 11.15]	1.81 (2.80) [-10.47, 18.08]	1.57 (2.15) [-7.25, 9.81]	0.85 (1.20) [-4.15, 1.96]	1.37 (1.88) [-3.35, 5.31]	1.70 (2.51) [-12.33, 18.08]
G4 <sup>a</sup>	1.95 (2.97) [-11.05, 11.73]	1.51 (2.32) [-10.75, 11.02]	1.40 (1.98) [-7.06, 9.16]	0.98 (1.25) [-3.87, 1.65]	1.13 (1.49) [-3.45, 3.47]	1.47 (2.19) [-11.05, 11.73]
ccCA <sup>b</sup>	2.15 (3.24) [-12.54, 10.50]	1.69 (2.42) [-9.60, 19.71]	1.58 (2.18) [-9.36, 8.67]	1.00 (1.27) [-2.52, 2.99]	1.59 (2.25) [-5.88, 1.03]	1.66 (2.37) [-12.54, 19.71]
CBS-QB3 <sup>c</sup>	6.29 (8.88) [-14.77, 31.23]	2.75 (3.41) [-15.99, 6.76]	2.32 (3.38) [-6.74, 17.25]	2.87 (4.39) [-17.03, 9.63]	1.70 (2.20) [-6.00, 2.82]	2.82 (4.17) [-17.03, 31.23]
PM6	7.81 (11.04) [-40.57, 24.09]	3.79 (5.36) [-11.99, 42.15]	3.10 (4.29) [-25.88, 19.44]	4.35 (5.21) [-8.52, 9.92]	12.88 (16.28) [-41.87, 37.50]	4.02 (6.10) [-41.87, 42.15]
PM7	9.34 (13.89) [-72.66, 32.44]	3.44 (4.58) [-16.95, 23.05]	2.83 (3.99) [-28.91, 15.79]	6.04 (9.29) [-14.44, 35.40]	11.93 (14.58) [-42.78, 25.76]	3.89 (6.26) [-72.66, 35.40]
BLYP	13.81 (18.50) [-51.31, 52.49]	39.02 (43.82) [-149.30, 6.68]	20.47 (25.84) [-146.46, 25.03]	7.77 (10.92) [-22.54, 30.66]	14.06 (20.92) [-64.24, 26.35]	26.33 (32.93) [-149.30, 52.49]
PW91	34.29 (49.66) [-5.30, 170.02]	44.01 (50.49) [1.25, 208.96]	41.36 (46.12) [-2.50, 122.40]	9.33 (15.54) [-7.05, 49.25]	24.77 (29.17) [-1.52, 62.29]	40.76 (47.43) [-7.05, 208.96]
PBE	32.91 (47.46) [-9.61, 160.27]	39.21 (46.34) [-0.14, 203.43]	37.78 (42.85) [-5.56, 119.47]	9.64 (15.49) [-10.63, 49.36]	22.93 (27.18) [-3.16, 62.86]	37.03 (43.97) [-10.63, 203.43]
TPSS	7.70 (10.76) [-29.71, 35.52]	4.74 (5.82) [-32.48, 14.14]	4.67 (5.86) [-33.81, 20.80]	5.92 (7.58) [-13.19, 18.41]	6.58 (7.36) [-7.33, 12.68]	5.03 (6.50) [-33.81, 35.52]
B3LYP	14.12 (21.47) [-75.59, 11.64]	20.43 (23.70) [-90.90, 1.81]	13.57 (16.39) [-93.17, 4.88]	4.45 (6.50) [-19.02, 11.39]	6.99 (11.16) [-37.63, 5.75]	15.83 (19.65) [-93.17, 11.64]
B3LYP-D3	8.30 (11.70) [-41.04, 12.76]	3.92 (4.88) [-15.05, 25.03]	3.87 (4.99) [-15.47, 18.67]	3.94 (5.30) [-13.47, 13.17]	3.83 (4.46) [-7.07, 10.18]	4.28 (5.86) [-41.04, 25.03]
O3LYP	38.29 (58.65) [-3.92, 213.59]	97.05 (102.99) [9.64, 290.86]	75.24 (81.19) [6.70, 225.99]	13.00 (17.22) [-1.20, 46.75]	43.80 (53.68) [4.25, 110.02]	78.16 (87.13) [-3.92, 290.86]
X3LYP	13.30 (19.84) [-68.30, 9.42]	19.69 (22.66) [-85.66, 1.53]	13.38 (15.95) [-88.04, 3.91]	4.46 (6.46) [-19.95, 9.18]	6.64 (10.68) [-35.65, 5.33]	15.38 (18.84) [-88.04, 9.42]
PBE0	6.49 (8.92) [-18.56, 38.08]	12.82 (17.76) [-2.48, 88.73]	8.83 (12.26) [-16.21, 46.93]	5.44 (6.33) [-15.11, 8.19]	6.87 (9.79) [-2.75, 33.17]	9.99 (14.20) [-18.56, 88.73]
TPSS0	23.28 (34.13) [-125.62, 7.54]	7.66 (11.73) [-69.95, 7.76]	13.90 (17.23) [-62.70, 10.29]	9.91 (12.90) [-38.63, 18.55]	6.68 (8.23) [-17.41, 11.55]	12.20 (17.53) [-125.62, 18.55]
TPSS0-D3	18.42 (27.05) [-99.14, 9.67]	10.91 (12.29) [-18.31, 37.22]	8.46 (10.77) [-34.21, 38.28]	9.78 (12.51) [-34.45, 22.95]	8.33 (9.77) [-16.11, 20.44]	10.26 (13.55) [-99.14, 38.28]
M06-2X	5.06 (7.16) [-22.04, 26.54]	6.47 (7.54) [-26.66, 5.36]	3.68 (4.76) [-22.14, 13.07]	3.07 (3.89) [-9.23, 3.40]	3.29 (4.55) [-13.18, 3.85]	4.81 (6.13) [-26.66, 26.54]
M06-2X-D3	5.12 (7.30) [-22.04, 27.65]	6.03 (7.02) [-23.80, 5.47]	3.49 (4.53) [-22.12, 13.16]	3.07 (3.88) [-9.23, 3.40]	3.20 (4.43) [-13.18, 3.85]	4.55 (5.82) [-23.80, 27.65]
$\omega$ B97X	3.84 (5.11) [-19.25, 13.03]	3.58 (4.46) [-21.79, 8.71]	2.45 (3.37) [-19.45, 10.52]	2.60 (3.27) [-8.30, 6.35]	2.15 (2.96) [-7.62, 7.48]	2.98 (3.97) [-21.79, 13.03]
$\omega$ B97X-D3	4.02 (5.36) [-18.74, 11.73]	3.34 (4.09) [-18.75, 8.78]	2.35 (3.20) [-18.71, 7.45]	2.64 (3.34) [-7.37, 6.41]	2.02 (2.81) [-7.09, 7.27]	2.86 (3.77) [-18.75, 11.73]
$\omega$ B97X-V	5.08 (7.60) [-12.28, 34.23]	2.49 (3.37) [-15.74, 15.32]	2.94 (3.91) [-11.97, 17.44]	3.10 (3.82) [-5.49, 9.93]	2.98 (3.73) [-7.00, 10.20]	2.97 (4.19) [-15.74, 34.23]
$\omega$ B97X-D3BJ	4.73 (6.79) [-17.09, 29.03]	3.58 (4.28) [-18.15, 8.38]	2.50 (3.21) [-11.15, 13.37]	3.93 (4.92) [-5.53, 15.07]	2.10 (3.01) [-7.35, 6.52]	3.11 (4.08) [-18.15, 29.03]
$\omega$ B97M-V <sup>d</sup>	7.90 (11.43) [-13.00, 46.15]	15.76 (17.08) [-0.15, 55.99]	12.63 (13.95) [-11.22, 43.64]	3.34 (4.32) [-1.89, 10.78]	7.35 (9.10) [-6.59, 21.09]	13.12 (14.83) [-13.00, 55.99]
$\omega$ B97M+D3BJ <sup>d</sup>	3.98 (5.40) [-20.41, 17.12]	9.25 (9.98) [-1.36, 34.11]	6.73 (7.84) [-19.05, 23.61]	2.83 (3.57) [-5.11, 10.05]	4.48 (5.48) [-9.78, 12.10]	7.32 (8.45) [-20.41, 34.11]
CAM-B3LYP	6.78 (9.54) [-36.71, 14.17]	3.84 (5.84) [-30.74, 5.52]	3.92 (5.49) [-30.10, 12.42]	3.50 (4.47) [-12.86, 7.13]	3.89 (4.49) [-10.69, 6.87]	4.14 (6.05) [-36.71, 14.17]
B2PLYP	5.89 (8.34) [-27.80, 11.03]	7.29 (9.20) [-39.18, 12.71]	4.96 (6.32) [-35.64, 12.16]	2.76 (3.75) [-9.29, 10.69]	3.30 (4.82) [-15.88, 5.93]	5.82 (7.63) [-39.18, 12.71]
B2PLYP-D3	3.68 (5.06) [-14.77, 18.46]	4.43 (7.24) [-11.53, 46.82]	3.96 (5.56) [-8.73, 23.97]	2.37 (3.26) [-6.77, 11.46]	2.11 (2.79) [-2.22, 9.29]	4.04 (6.12) [-14.77, 46.82]
mPW2PLYP-D	4.93 (6.44) [-19.63, 11.68]	4.11 (5.38) [-6.42, 30.59]	3.14 (4.04) [-14.16, 18.05]	2.86 (3.63) [-11.42, 6.79]	2.09 (2.70) [-4.97, 6.76]	3.63 (4.79) [-19.63, 30.59]

<sup>a</sup> Nonhydrogens: 141, Hydrocarbons: 615, Subst. hydrocarbons: 849, Total: 1674

<sup>b</sup> Nonhydrogens: 146, Hydrocarbons: 551, Subst. hydrocarbons: 805, Total: 1571

<sup>c</sup> Nonhydrogens: 147, Hydrocarbons: 621, Total: 1689

<sup>d</sup> Nonhydrogens: 139, Inorganic hydrides: 28, Total: 1681

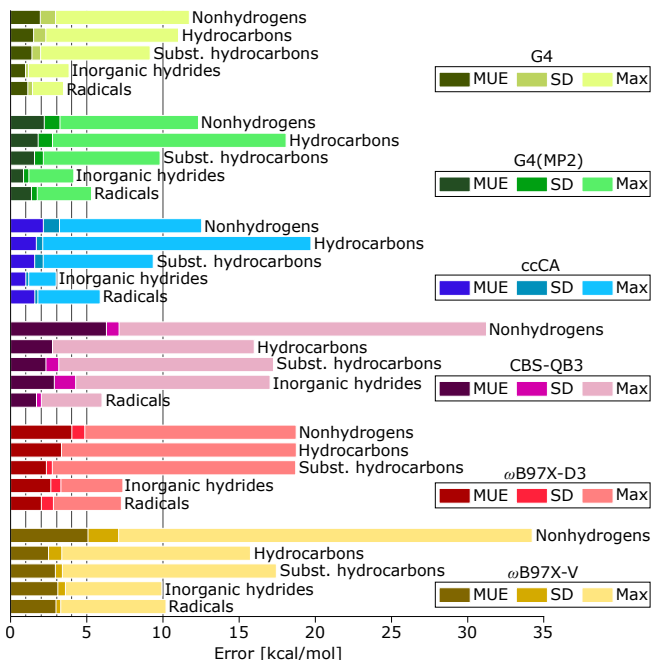


FIG. 6. Prediction errors in  $\Delta H_f^o$  across compound types and methods; MUE: mean unsigned error, SD: standard deviation, Max: maximum absolute deviation. For number of entries in each class of compounds and methods, see Table. I

errors for each method across various classes of compounds in PPE1694. It is apparent while moving across various subsets, that the performance of cWFTs – G4, G4(MP2), and ccCA – are consistent irrespective of the compound type, with MUEs below 2 kcal/mol, while CBS-QB3 performs poorly with larger deviations relative to the other cWFTs particularly in the case of Nonhydrogens.

We note the GGA functionals to consistently underperforming across all subsets. A closer look reveals errors to be mostly systematic as higher MUEs are usually encountered for subsets with greater structural complexities. Hybrid GGAs mostly improve upon GGA results (barring O3LYP), by accounting for better approximations of the dispersion interactions. Overall, as we move up the *Jacob’s ladder*<sup>47</sup>, we observe a consistent drop in MUE. Most notably, we find the long-range tuned hybrid DFAs to perform better than double hybrids DFAs. The importance of capturing long-range effects can be further understood by noting that explicit inclusion of an empirical dispersion correction mostly improves the performance across DFAs. Semi-empirical methods PM6 and PM7 under-perform across all subsets except in the case of hydrocarbons, where their accuracy is on par with long-range tuned functionals with PM7 slightly outperforming PM6. For the six best performing methods: G4, G4(MP2), ccCA, CBS-QB3,  $\omega$ B97X-D3, and  $\omega$ B97X-V, we have graphically summarized the error metrics in Fig. 6. As noted

before in Table. I, G4 ranks the highest followed by G4(MP2) and ccCA exhibiting comparable prediction accuracies. In terms of the maximum absolute deviation (Max), ccCA seems slightly better than G4 & G4(MP2) for inorganic hydrides. Amongst the DFAs,  $\omega$ B97X-D3 shows reduced Max than  $\omega$ B97X-V consistently barring (un)substituted hydrocarbons; both yields large Max values for (un)substituted hydrocarbons, which we believe to stem from the lack of such compounds in the training of these DFAs.

A drawback of relying on mean-based error metrics is that, these do not provide a complete picture of the error distribution. For this purpose, percentile-based metrics have been shown to be more suitable (see Ref. 104 and references therein). Fig. 7 presents mean- and percentile-based metrics for all the computational methods studied here. A method with good prediction accuracy should show smaller MUEs as well as small values of  $Q_N$ , where  $N > 50$ . Spearman rank correlation ( $\rho$ ) between two sets is a good indicator for qualitative agreement between them<sup>114</sup>. Compared to 1694 experimental  $\Delta H_f^o$  values, we find G4, G4(MP2) and ccCA to show a strong correlation amounting to  $\rho = 0.999$ . For the DFAs, we find dispersion corrections to mostly improve  $\rho$ . In fact, although  $\omega$ B97X-D3 and CBS-QB3 show similar MUE, the dispersion corrections allow the DFA to present a slightly superior  $\rho$  to that of CBS-QB3. As noted for MUE, the percentile metrics and the  $\rho$  of the semi-empirical methods PM6 and PM7 are consistently superior than that of the GGA methods. This is because these simple methods have been trained to deliver accurate values of  $\Delta H_f^o$  for hydrocarbons and substituted hydrocarbons that also dominate the PPE1694 dataset.

The apparent success of dispersion corrected DFAs motivated us to have a closer look at the effect basis set size has on accuracy. To this end, we have collected  $\Delta H_f^o$  values for the 459 systems in the Pedley CHONF dataset (see Section IV) and studied these with def2-XVP (X=S, TZ, and QZ) basis sets using B3LYP and  $\omega$ B97X DFAs—with and without a D3 term (see Table II). Among all possibilities, we note the performance to be the best for  $\omega$ B97X-D3 with a QZ basis set. This result is in accord with the findings reported in Ref. 5. Fortuitously, B3LYP achieves minimum error for the smallest basis set, indicating an inconsistent trend in accuracy with basis set size—a trend also noted in Ref. 39. However, we find the D3-corrected B3LYP to somewhat improve this situation. When going from B3LYP to B3LYP-D3, we note a larger gain in accuracy with the QZ basis set; however, for the  $\omega$ B97X DFA, D3 term only leads to a modest improvement so long as the basis set is QZ.

Examining the compounds showing extreme (*i.e.* most-positive or most-negative) errors for a given computational method often reveals if the error is systematic or non-systematic in nature. For the latter to be evident one has to consider normalized or intensive errors such as error-per-electron or error-per-

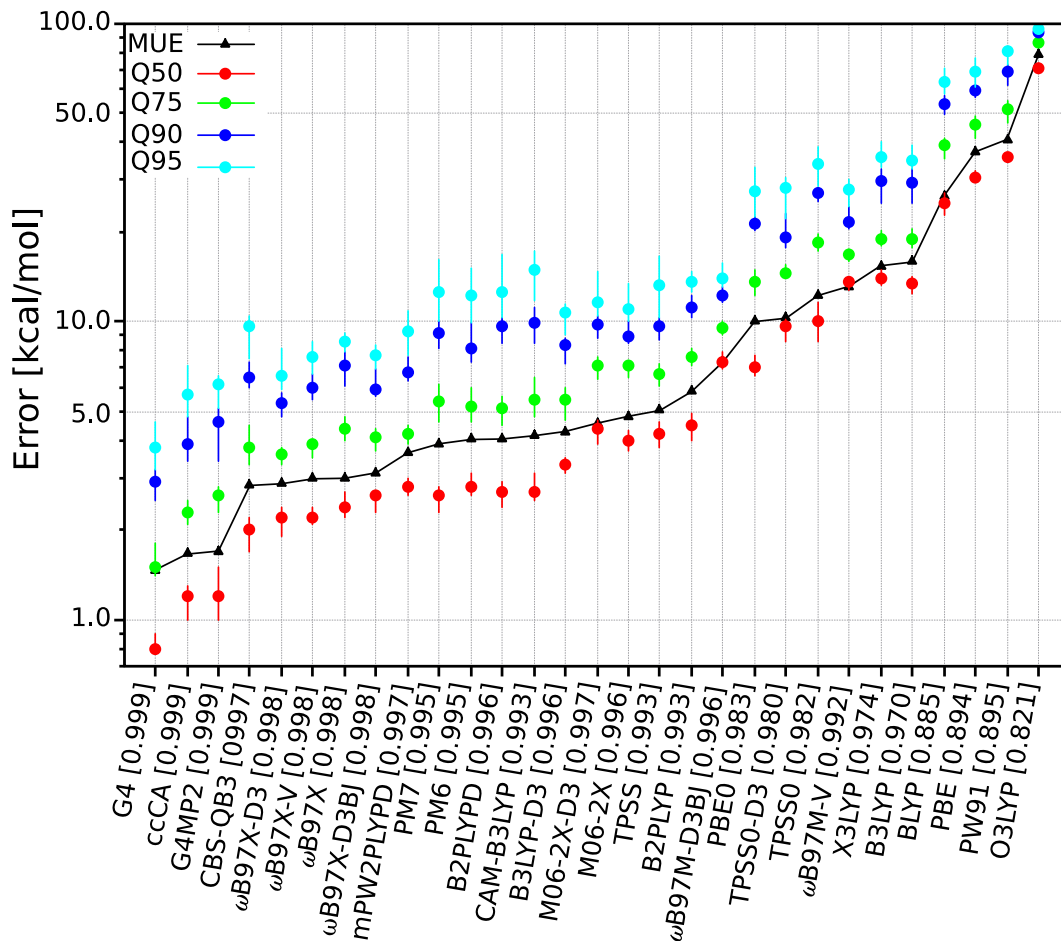


FIG. 7. Ranking of the prediction accuracy of cWFTs, DFAs and semi-empirical models. For each method, the mean unsigned error (MUE) and cumulative probability percentiles,  $Q_n$  ( $n = 50, 75, 90$ , and  $95$ ) are reported in log-scale. Methods are sorted in ascending order of MUE. Values in square brackets are the Spearman rank correlations w.r.t experimental values. Vertical lines on the percentile points denote the standard deviation estimated via bootstrapping.

TABLE II. Dependence of prediction accuracy of B3LYP and  $\omega$ B97X DFAs on the D3 empirical dispersion correction and def2-XVP ( $X = S/TZ/QZ$ ) basis sets. For a given DFA and basis set, MUE in the predicted  $\Delta H_f^\circ$  is reported when compared to experimental values. The benchmark dataset comprises 459 molecules (“Pedley CHONF dataset”) with 175 hydrocarbons and 284 substituted hydrocarbons. All values are reported in kcal/mol.

Dataset	B3LYP			B3LYP-D3			$\omega$ B97X			$\omega$ B97X-D3		
	S	TZ	QZ	S	TZ	QZ	S	TZ	QZ	S	TZ	QZ
Hydrocarbons (175)	2.69	16.42	13.69	15.54	1.75	2.93	12.65	4.26	2.24	12.72	4.47	2.18
Subs. hydrocarbons (284)	5.06	11.71	9.23	16.06	2.84	3.79	11.95	3.49	1.74	11.98	3.56	1.71
Total (459)	4.16	13.51	10.93	15.86	2.42	3.46	12.22	3.78	1.93	12.26	3.91	1.89

atom. In the case of G4(MP2), along with the total error, we also consider error-per-valence-electron and inspected those compounds exhibiting extreme errors (see Fig. 8). Barring the hydrocarbons category, we find the compounds with extreme intensive and extensive (*i.e.* unnormalized) error to mostly comprise heavy atoms. Predominant of the compounds with large intensive error are with fewer heavy atoms, while those with large extensive (or unnormalized) error consist of either a large number of atoms or contain sev-

eral heavy atoms. Hydrocarbons cycloheptadecane and 9,10-diphenylanthracene feature the largest extensive error; from opposite signs of the errors of these two compounds, one may speculate that the source of their errors cannot be due to the uncertainties associated with the parameters used in the enthalpy evaluation (see Section VID for a discussion). A specialized study on these extreme compounds displayed in Fig. 8 with more robust cWFTs or WFTs should reveal further insights into both, the deficiencies of G4(MP2) in modeling the  $\Delta H_f^\circ$  of

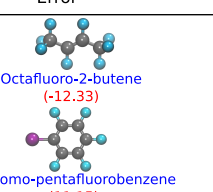
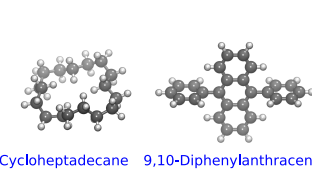
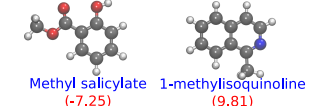
	Error	Error per Valence Electron
Non-Hydrogens	 <p>Octafluoro-2-butene (-12.33)</p> <p>1-Bromo-pentafluorobenzene (11.15)</p>	 <p>Dilithium (-0.74)</p> <p>Calcium Oxide (0.37)</p>
Hydrocarbons	 <p>Cycloheptadecane (-10.47)</p> <p>9,10-Diphenylanthracene (18.08)</p> <p>Bicyclo[3.3.1]nonane (-0.14)</p> <p>(15,25)-1,2-dimethylcyclobutane (0.15)</p>	
Subst. Hydrocarbons	 <p>Methyl salicylate (-7.25)</p> <p>1-methylisoquinoline (9.81)</p>	 <p>Trimethylaluminum (-0.19)</p> <p>Vinyl chloride (0.22)</p>
Inorganic hydrides	 <p>Dihydrogen sulfate (-4.15)</p> <p>Disilane (1.96)</p>	 <p>Hydroxylamine (-0.16)</p> <p>Silylene (0.26)</p>
Radicals	 <p>Butanoyloxidanyl (-3.35)</p> <p>Cubyl (5.31)</p>	 <p>Chlorine monoxide (-0.11)</p> <p>Silyl (0.26)</p>

FIG. 8. Left column presents molecules in the PPE1694 dataset exhibiting the highest deviations in G4(MP2) predicted  $\Delta H_f^\circ$ . Right column shows molecules with extreme errors per valence electron.

these systems, and also clarify the uncertainties in the experimental results.

It is important to compare the accuracy of the G4(MP2) and ccCA results presented above, based on the present implementation, to that of legacy implementations of these cWFTs. Firstly, all our calculations are based on a framework employing spherical primitive Gaussian type orbitals (GTOs), while Pople basis sets—used for B3LYP geometry relaxation, and G4(MP2) energies—are conventionally used in the Cartesian primitive GTO framework. Secondly, the ccCA-P<sup>38</sup> formalism uses B3LYP/cc-pVTZ reference geometry with Hartree-Fock and MP2 energies extrapolated separately to the CBS limit, relativistic DKH2 corrections for open-shell molecules calculated with a spin-collinear (*i.e.* UHF) reference wavefunction, and employs a different scale factor for ZPVE. To this end, in Table III, we compare prediction errors in our cWFT calculations for the entire G3/05 dataset to that of previously published results with same methods. For comparison, we have also summarized previous results based on the more accurate G4 theory.

As far as the G4(MP2) results are concerned, going from Cartesian GTOs to spherical GTOs leads to a tiny increase in the MUE by 0.01 kcal/mol. Our prediction error for ccCA fares rather well when com-

TABLE III. Comparison between errors in G4(MP2), ccCA and G4 for G3/05 and Pedley CHONF. Both results from previous and current studies are included for all classes of compounds.

Dataset	G4(MP2)	ccCA	G4
I. G3/05 (452) <sup>a</sup>	1.05, 1.04 <sup>b</sup>	0.98, 0.99 <sup>c</sup>	0.83 <sup>d</sup>
1. $\Delta H_f^\circ$ (270)	1.00, 0.99 <sup>b</sup>	0.93, 0.95 <sup>c</sup>	0.80 <sup>d</sup>
-Nonhydrogens (79)	1.46, 1.44 <sup>b</sup>	1.04	1.13 <sup>d</sup>
-Hydrocarbons (38)	0.64, 0.63 <sup>b</sup>	0.96	0.48 <sup>d</sup>
-Subst. Hydrocarbons (100)	0.84, 0.83 <sup>b</sup>	0.85	0.68 <sup>d</sup>
-Inorganic hydrides (19)	0.92, 0.94 <sup>b</sup>	0.99	0.92 <sup>d</sup>
-Radicals (34)	0.83, 0.86 <sup>b</sup>	0.82	0.66 <sup>d</sup>
2. IP (103) <sup>a</sup>	1.08, 1.07 <sup>b</sup>	1.08, 1.09 <sup>c</sup>	0.91 <sup>d</sup>
-Atoms (26)	1.12, 1.13 <sup>b</sup>	0.55	0.65 <sup>d</sup>
-Molecules (77)	1.06, 1.05 <sup>b</sup>	1.26	0.99 <sup>d</sup>
3. EA (63)	1.26, 1.23 <sup>b</sup>	0.97, 1.03 <sup>c</sup>	0.83 <sup>d</sup>
-Atoms (14)	1.86, 1.84 <sup>b</sup>	0.89	0.91 <sup>d</sup>
-Molecules (49)	1.10, 1.06 <sup>b</sup>	1.00	0.81 <sup>d</sup>
4. PA (10)	0.66, 0.67 <sup>b</sup>	1.23, 0.93 <sup>c</sup>	0.84 <sup>d</sup>
5. BE (6)	1.29, 1.28 <sup>b</sup>	1.15, 0.58 <sup>c</sup>	1.12 <sup>d</sup>
II. Pedley, $\Delta H_f^\circ$ (459)	0.78, 0.79 <sup>e</sup>	1.01	
-Hydrocarbons (175)	0.61, 0.68 <sup>e</sup>	0.88	
-Subst. hydrocarbons (284)	0.88, 0.86 <sup>e</sup>	1.08	

<sup>a</sup> We have excluded two triplet entries for H<sub>2</sub>S and N<sub>2</sub>

<sup>b</sup> from Ref. 37

<sup>c</sup> from Ref. 38

<sup>d</sup> from Ref. 23

<sup>e</sup> from Ref. 5

pared to ccCA-P values from Ref. 38, while the original formalism—with a larger basis set for geometry optimization—showing much smaller error for the binding energy of hydrogen bonded dimers. We believe that the accuracy of our ccCA results can improve when adopting the ccCA settings to be similar to that of the ccCA-P<sup>38</sup> implementation, however, here we have used settings that will render the comparison between G4(MP2) and ccCA seamless.

Further, we have extended the comparison between cWFTs to the slightly larger dataset – Pedley CHONF (see Section IV); we note our G4(MP2) results to agree fairly well with that of previously reported values from Ref. 5. Interestingly, for G4(MP2) we find the accuracies for hydrocarbons and their substituted analogues to be retained when going from the G3/05 set to Pedley CHONF. As for ccCA, the MUE of 1.01 kcal/mol for the Pedley CHONF dataset is comparable to that of the total error for the G3/05 set, indicating the small deviations in both values to lie within the uncertainties in the reference experimental values.

## B. Role of HLC in G4(MP2) and its Transferability across Datasets

An interesting point of concern in the  $G_n$ -series of cWFTs—more specifically G4(MP2)—is the role HLC plays in the model (see Eq. 5). To gain more insight

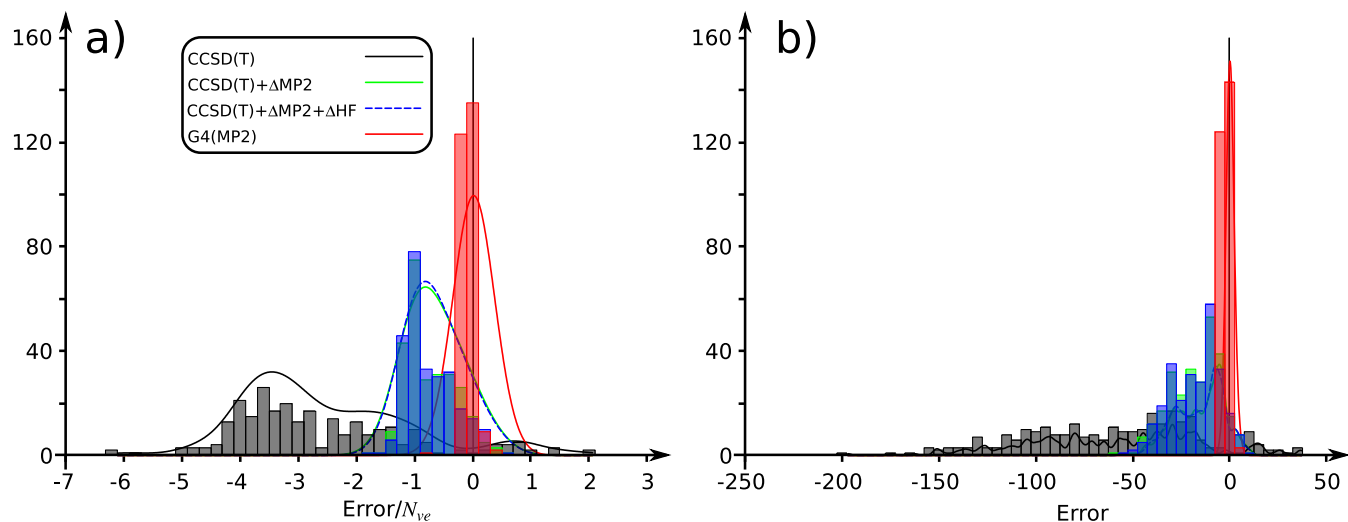


FIG. 9. Effect of systematic inclusion of components in the G4(MP2)  $\Delta H_f^\circ$  on error distribution; SO, ZPVE and thermal corrections have been included in all calculations. For 270 molecules from the G3/05 dataset, error distribution of predicted  $\Delta H_f^\circ$  are shown: a) per valence electron (*i.e.* Error/ $N_{ve}$ ), and b) without normalization. Black boxes stand for CCSD(T) values, green ones correspond to values with  $\Delta$ MP2 corrections, blue correspond to results with further inclusion of  $\Delta$ HF corrections, and the final G4(MP2) results with HLC are shown in red.

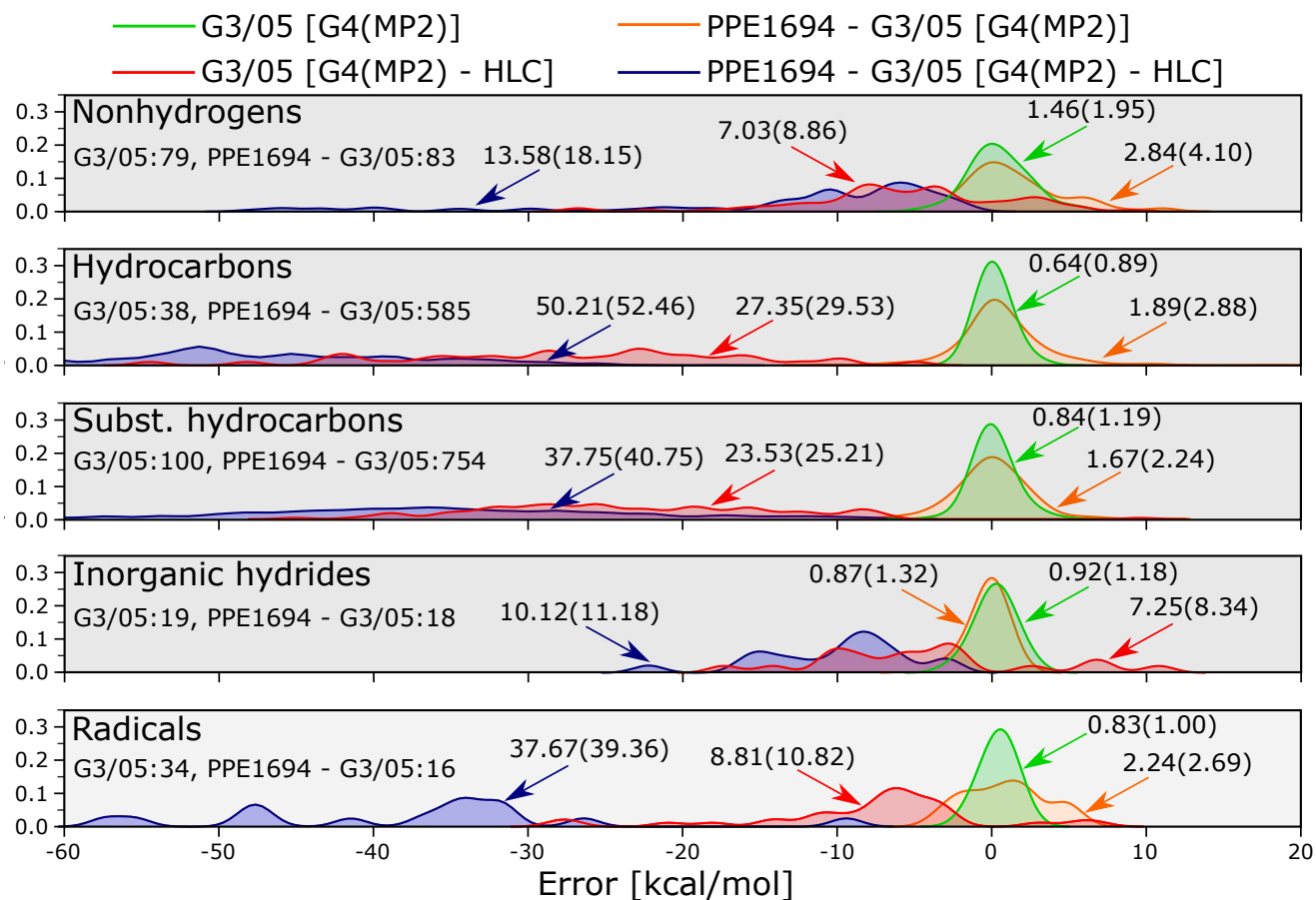


FIG. 10. Influence of HLC in determining  $\Delta H_f^\circ$  for various classes of compounds in the G3/05 dataset and rest of the compounds in the PPE1694 dataset. For both sets, results are shown separately with and without the HLC term. The arrows point to MUE (RMSE) for each error distribution. The lower bound of the error is set to -60 kcal/mol for clarity.

on this point, we present the error in G4(MP2) predic- tions with successive inclusion of energy terms in Fig. 9

for the case of 270  $\Delta H_f^\circ$  values from the G3/05 set. The distributions are shown for both extensive and intensive errors.

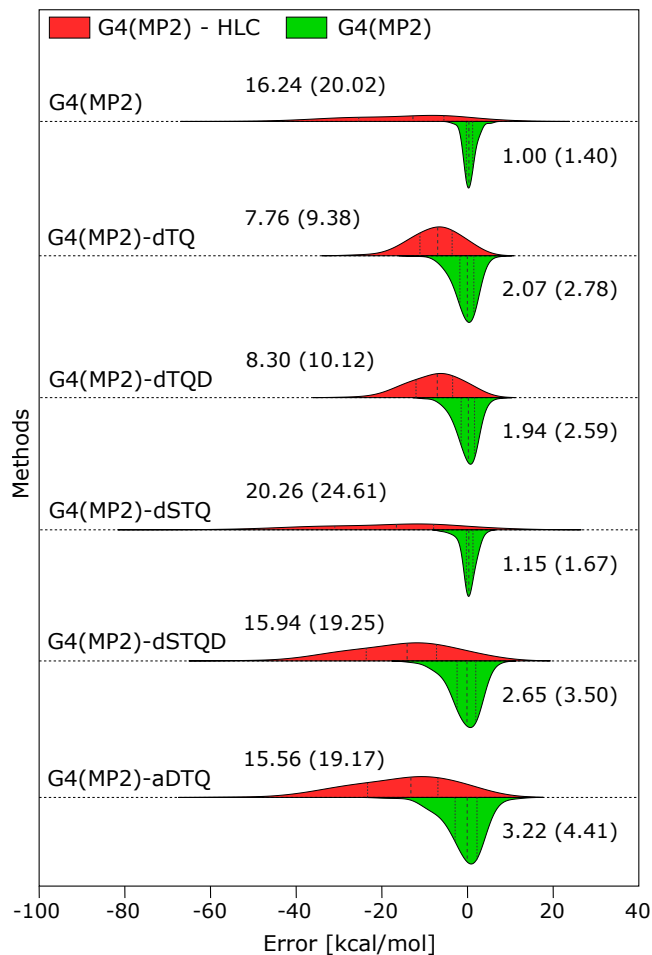


FIG. 11. Distribution of prediction errors for the G3/05 dataset, with and without reoptimized HLC. For 270  $\Delta H_f^\circ$  values, results are shown for variants of G4(MP2) based on different basis sets. See Table IV for more details.

In both cases, the CCSD(T) error distribution is broad and multimodal, narrowing with successive inclusion of  $\Delta$ MP2 and  $\Delta$ HF corrections. The error in the resulting model exhibits a spread: -50 kcal/mol to 10 kcal/mol for the extensive errors, which is quenched by the inclusion of the HLC term. It is remarkable that the HLC term, given its simple form, not only shifts the error distribution to center at zero, but also changes the shape of the distribution. This indicates the HLC term to account for both systematic and non-systematic corrections. While the contributions from  $\Delta$ HF seems negligible, excluding this term in the G4(MP2) energy deteriorates the MUE for the 270 values of  $\Delta H_f^\circ$  from 1.00 kcal/mol to 1.36 kcal/mol. Reoptimizing the HLC term without the HF corrections takes the MUE to 1.18 kcal/mol, still deviating from the G4(MP2) value by 0.19 kcal/mol.

Having observed the influence of HLC on 270  $\Delta H_f^\circ$ s in

G3/05, we investigate its transferability across various classes of compounds in G3/05 and PPE1694 (Fig. 10). HLC for nonhydrogens reduces MUE  $\approx$  5-times for both G3/05 as well the remaining nonhydrogens in PPE1694. G3/05 hydrocarbons, show a 43-fold decay in MUE without the HLC correction while the decay is 27-fold for the remaining ones in PPE1694. Drop in MUE is 28- and 23-fold for substituted hydrocarbons in G3/05 and the rest in PPE1694, respectively. For inorganic hydrides, MUE drops 8-fold for G3/05, while it is 12-fold for others in PPE1694. Radicals show a 11-fold decay in MUE for G3/05 while the rest in PPE1694 show a 17-fold drop. Though HLC captures systematic and non-systematic effects successfully across compound types and datasets, we do note the quantitative prediction accuracy of G4(MP2) to drop from 1.00 kcal/mol to 1.70 kcal/mol, when going from the G3/05 dataset (Table III) to the PPE1694 set (Table I). This drop in accuracy when increasing the dataset size may be ascribed to both the residual uncertainties in the experimental results, and also the systematic error introduced in the form of empirical reference data for atoms, forms the subject of Section VID.

The original motivation to add a HLC term in the G1 theory<sup>85</sup> was to account for the remaining basis set errors in the model. It has been noted that a successful performance of the method requires the finite basis sets employed at various levels be “balanced”<sup>85</sup>. To probe the sensitivity of HLC to the choice of basis set, we replaced the Pople basis sets used in G4(MP2) with Dunning or Karlsruhe basis sets and re-parameterized all components in HLC by training on the G3/05 dataset; see Eq. 6 for the definitions. The resulting parameters are presented in Table IV. As expected, when moving from the default G4(MP2) basis sets to larger Karlsruhe sets (dTQ and dTQD series in Table IV), we find the magnitude of the all HLC parameters barring E to drop indicating less dependence of the accuracy on the HLC term; this trend is reminiscent of the fact that going from G4(MP2) to G4<sup>23</sup>, the magnitude of the HLC parameters decrease. This, however, does not necessarily lead to any increase in the method’s accuracy, as G4(MP2)-dTQD’s MUE increases to 1.94 kcal/mol. Among the tested variants, the one using the smallest basis sets, G4(MP2)-dSTQ, shows the HLC parameters of larger magnitudes. Surprisingly, we find this variant to have an MUE of 1.15 kcal/mol, which is much smaller than that of G4(MP2)-dTQD. The method suffers maximum deterioration when using the aug-cc-pVXZ basis sets (def2-SVPD/TZVPPD/QZVPPD basis sets for K and Ca), resulting in an MUE of 3.22 kcal/mol. These results indicate that successfully exploiting the form of the HLC term, also requires careful tailoring of the basis sets used for the CCSD(T), MP2 and HF energies. For the variants tried, we have presented the error distributions with and without the HLC contributions, in Fig.11.

TABLE IV. HLC parameters for the G4(MP2) method using various basis sets trained on the G3/05 dataset. For each variant the mean unsigned error (MUE) is also given.

Method	HLC parameters ( $mE_H$ )						MUE (kcal/mol)
	A	A'	B	C	D	E	
G4(MP2)	9.472	3.102	9.741	2.115	9.769	2.379	1.00
G4(MP2)-dTQ <sup>a</sup>	7.87463	3.68724	7.32518	3.13840	8.13897	2.67364	2.07
G4(MP2)-dTQD <sup>b</sup>	4.97612	1.95851	4.51679	1.53565	5.17235	6.40621	1.94
G4(MP2)-dSTQ <sup>c</sup>	10.16067	2.94668	10.26727	1.95410	10.44012	2.25370	1.15
G4(MP2)-dSTQD <sup>d</sup>	9.29772	2.68841	8.63923	2.65558	9.65029	2.34433	2.65
G4(MP2)-aDTQ <sup>e</sup>	5.54878	1.44401	4.91740	0.81254	5.74020	1.45242	3.22

<sup>a</sup> CCSD(T)/def2-TZVP, MP2/def2-QZVP, HF/CBS(def2-TZVP,def2-QZVP)

<sup>b</sup> CCSD(T)/def2-TZVPPD, MP2/def2-QZVPPD, HF/CBS(def2-TZVPPD,def2-QZVPPD)

<sup>c</sup> CCSD(T)/def2-SVP, MP2/def2-TZVP, HF/CBS(def2-TZVP,def2-QZVP)

<sup>d</sup> CCSD(T)/def2-SVPD, MP2/def2-TZVPPD, HF/CBS(def2-TZVPPD,def2-QZVPPD)

<sup>e</sup> CCSD(T)/aug-cc-pVDZ, MP2/aug-cc-pVTZ, HF/CBS(aug-cc-pVTZ,aug-cc-pVQZ)

### C. ISO32 dataset for isomerization reaction energies

Accurate prediction of isomerization energies is one of the stringent tests for testing the reliability of WFTs, cWFTs and DFAs<sup>115</sup> since isomerization reaction energetics exclusively encode information about orbital hybridization, electronic conjugation and steric effects in chemical bonding<sup>116,117</sup>. Previous studies have observed majority of the DFAs to predict qualitatively incorrect trends for the energy ordering of constitutional isomers belonging to a stoichiometry<sup>118</sup>. From the point of view of thermochemical procedures, all systematic contributions to molecular enthalpies such as empirical atomic corrections, and HLC are cancelled in isomerization energies. Hence, prediction errors expose non-systematic errors encoded in the evaluation of electronic energies. To identify a large benchmark suite of isomerization energies, we collected constitutional isomers belonging to 32 unique stoichiometries in the PPE1694 dataset amounting to 517 unique systems, labelling this subset as ISO32. ISO32 contains stoichiometries with  $\geq 7$  systems where for constitutional isomers with same  $\Delta H_f^{\circ, \text{exp}}$ , only the system with lowest  $\Delta H_f^{\circ, \text{G4(MP2)}}$  was kept.

Table V presents, for each stoichiometry, mean errors in the prediction of isomerization energies where the reactant is the global minimum in each set, amounting to 485 reaction energies. For ccCA,  $\Delta H_f^{\circ}$  for 1, 3 and 1 systems were missing for stoichiometries  $\text{C}_8\text{H}_{14}$ ,  $\text{C}_9\text{H}_{16}$  and  $\text{C}_9\text{H}_{18}$  respectively, thus, resulting in 480 reaction energies only. In terms of prediction accuracy, the cWFTs are found to perform better than DFTs, with ccCA providing the smallest MUE of 1.86 kcal/mol, while the largest MUE being 2.63 kcal/mol for  $\omega\text{B97X-V}$ . Interestingly, CBS-QB3 shows similar prediction accuracy to G4, both of which are followed by G4(MP2) in evaluating isomerisation energies. Spearman rank correlation ( $\rho$ ) w.r.t experimental values, provides an important insight—the trends in  $\Delta H_f^{\circ}$  is mostly preserved across all meth-

ods. This may be speculated to be a consequence of the geometry of the molecules being optimized at same level of theory—B3LYP/6-31G(2df,p). Both MUE and  $\rho$  are essential to identify the efficiency of a method as  $\text{C}_{10}\text{H}_{10}$  presents the largest errors but also a perfect  $\rho$  suggesting the errors in this set to be systematic. However,  $\text{C}_8\text{H}_{18}$  presents a small MUE and  $\rho$  suggesting fortuitous error cancellation.

For all global minima in ISO32, we collected their error metrics in table VI. In table V, as per MUE ccCA  $< \text{G4} \approx \text{CBS-QB3} < \text{G4(MP2)} < \omega\text{B97X-D3} < \omega\text{B97X-V}$  while in table VI the observed trend is  $\text{G4} < \text{ccCA} < \text{G4(MP2)} < \text{CBS-QB3} < \omega\text{B97X-V} < \omega\text{B97X-D3}$ . The discrepancy in prediction accuracy trends across the isomerization energies and global minima can be explained upon noting that the former property accounts for non-systematic method-dependent errors better. Interestingly,  $\omega\text{B97X-V}$  consistently over-stabilizes the global minima, while  $\omega\text{B97X-D3}$  mostly destabilizes. Although this aids in improving  $\omega\text{B97X-V}$ 's prediction of  $\Delta H_f^{\circ}$  of (1R,2R,3S)-1,2,3-trimethylcyclopentane, where all other methods present poorer results—the success is transient. Thus, testing on isomerization energies—both trend and accuracy—during the method development should be beneficial towards improving prediction accuracy.

### D. Source of Systematic Errors in Molecular Standard Formation Enthalpies

Molecular  $\Delta H_f^{\circ}(298 \text{ K})$  depends on enthalpies of constituent atoms in their standard elemental forms. The absolute enthalpies per atom for the elements enter the calculation as empirical constants:  $\Delta H_f^{\circ}(0 \text{ K})$ , which is the zero-Kelvin enthalpy of formation per atom along with an associated thermal correction,  $H^{\circ}(298 \text{ K}) - H^{\circ}(0 \text{ K})$ . The former quantity contributes predominantly to the total energy, hence any uncertainty in their determination will be accrued with increasing molec-

TABLE V. Accuracies of G4, G4(MP2), ccCA, CBS-QB3,  $\omega$ B97X-D3 and  $\omega$ B97X-V for the prediction of isomerization enthalpies for 32 sets of constitutional isomers: MUE is mean unsigned error (in kcal/mol), RMSE is root-mean-square-error (in kcal/mol), and  $\rho$  is the Spearman rank correlation coefficient; the latter quantity is reported per stoichiometry.

Stoichiometry (#)	MUE (RMSE, $\rho$ )					
	G4	G4(MP2)	ccCA	CBS-QB3	$\omega$ B97X-D3	$\omega$ B97X-V
C <sub>4</sub> H <sub>6</sub> (7)	0.91 (1.13, 0.98)	1.03 (1.18, 0.98)	0.80 (1.02, 1.00)	0.96 (1.21, 0.98)	3.27 (3.88, 1.00)	3.63 (4.31, 1.00)
C <sub>5</sub> H <sub>8</sub> (12)	0.81 (0.89, 0.99)	0.85 (0.94, 0.98)	0.40 (0.60, 0.99)	0.51 (0.61, 0.99)	1.88 (2.34, 0.97)	2.87 (3.12, 0.98)
C <sub>5</sub> H <sub>10</sub> (11)	0.79 (0.86, 0.99)	0.86 (0.90, 0.99)	0.26 (0.37, 0.99)	0.52 (0.64, 0.99)	1.36 (1.44, 1.00)	1.95 (2.22, 1.00)
C <sub>6</sub> H <sub>8</sub> (8)	1.11 (1.18, 0.98)	1.14 (1.24, 0.98)	0.89 (1.03, 1.00)	1.05 (1.13, 0.98)	1.27 (1.48, 1.00)	2.00 (2.33, 1.00)
C <sub>6</sub> H <sub>10</sub> (26)	0.96 (1.47, 0.99)	1.02 (1.54, 0.99)	0.91 (1.35, 0.99)	0.92 (1.38, 0.99)	1.86 (2.26, 0.97)	2.79 (3.21, 0.97)
C <sub>6</sub> H <sub>12</sub> (26)	0.87 (1.59, 0.97)	0.88 (1.55, 0.96)	0.84 (1.43, 0.97)	0.84 (1.45, 0.97)	2.10 (2.40, 0.93)	2.90 (3.20, 0.92)
C <sub>7</sub> H <sub>8</sub> (9)	1.79 (2.01, 0.96)	1.64 (1.96, 0.96)	1.63 (1.88, 0.96)	0.94 (1.20, 0.96)	3.04 (3.56, 0.96)	4.15 (5.16, 0.96)
C <sub>7</sub> H <sub>12</sub> (31)	1.18 (1.50, 0.97)	1.30 (1.64, 0.97)	1.38 (1.68, 0.97)	1.48 (1.74, 0.97)	2.04 (2.56, 0.98)	3.73 (4.61, 0.98)
C <sub>7</sub> H <sub>14</sub> (39)	0.66 (0.86, 0.91)	0.70 (0.94, 0.91)	0.60 (0.77, 0.93)	0.65 (0.83, 0.92)	1.21 (1.42, 0.94)	2.59 (2.89, 0.94)
C <sub>7</sub> H <sub>16</sub> (8)	0.37 (0.62, 0.97)	0.37 (0.62, 0.98)	0.47 (0.62, 0.97)	0.38 (0.61, 0.98)	0.95 (1.20, 0.99)	0.71 (0.88, 0.97)
C <sub>8</sub> H <sub>10</sub> (15)	1.43 (1.73, 0.98)	1.41 (1.78, 0.98)	1.34 (1.64, 0.98)	1.33 (1.60, 0.98)	1.79 (2.55, 0.99)	3.11 (3.96, 0.97)
C <sub>8</sub> H <sub>14</sub> (14)	1.14 (2.25, 0.94)	1.18 (2.28, 0.95)	1.07 (2.19, 0.93)	1.10 (2.13, 0.94)	1.61 (2.52, 0.94)	2.64 (3.23, 0.93)
C <sub>8</sub> H <sub>16</sub> (77)	4.81 (4.98, 0.89)	5.04 (5.21, 0.88)	4.60 (4.76, 0.89)	4.54 (4.73, 0.89)	3.76 (3.99, 0.90)	2.58 (3.05, 0.90)
C <sub>8</sub> H <sub>18</sub> (17)	1.77 (2.17, 0.69)	1.83 (2.22, 0.69)	1.23 (1.60, 0.59)	1.56 (1.98, 0.72)	1.85 (2.30, 0.33)	1.34 (1.57, 0.46)
C <sub>9</sub> H <sub>10</sub> (7)	0.66 (0.80, 0.86)	0.75 (0.89, 0.86)	0.82 (0.94, 0.76)	0.90 (1.13, 0.93)	2.08 (2.26, 0.76)	3.31 (3.47, 0.76)
C <sub>9</sub> H <sub>12</sub> (13)	0.95 (1.23, 0.99)	1.34 (1.82, 0.99)	1.25 (1.56, 0.99)	1.29 (1.58, 1.00)	1.52 (2.79, 1.00)	2.12 (3.50, 0.99)
C <sub>9</sub> H <sub>16</sub> (9)	2.91 (3.63, 0.93)	2.96 (3.71, 0.93)	2.42 (3.57, 0.96)	2.89 (3.56, 0.94)	2.57 (3.45, 0.95)	2.66 (3.80, 0.95)
C <sub>9</sub> H <sub>18</sub> (11)	3.62 (3.91, 0.71)	3.59 (3.90, 0.71)	3.43 (3.78, 0.62)	3.55 (3.85, 0.71)	2.70 (3.21, 0.73)	2.99 (3.40, 0.74)
C <sub>10</sub> H <sub>10</sub> (10)	5.35 (5.91, 1.00)	5.51 (6.21, 1.00)	5.66 (6.17, 1.00)	5.97 (6.63, 1.00)	6.67 (7.58, 1.00)	6.79 (8.00, 1.00)
C <sub>10</sub> H <sub>16</sub> (9)	2.61 (3.14, 0.99)	2.32 (2.89, 0.99)	2.81 (3.15, 0.99)	3.01 (3.49, 0.99)	3.00 (3.28, 0.99)	5.54 (6.19, 0.99)
C <sub>7</sub> H <sub>9</sub> N(13)	1.08 (1.70, 0.99)	1.10 (1.98, 0.99)	1.23 (2.02, 0.99)	1.32 (2.14, 0.99)	1.15 (2.40, 0.99)	1.10 (1.68, 0.99)
C <sub>5</sub> H <sub>10</sub> O(11)	0.50 (0.64, 0.99)	0.45 (0.56, 0.99)	0.56 (0.71, 0.98)	0.71 (0.97, 0.97)	0.99 (1.16, 0.97)	1.30 (1.50, 0.91)
C <sub>5</sub> H <sub>12</sub> O(11)	0.64 (1.18, 0.93)	0.66 (1.24, 0.91)	0.68 (1.20, 0.93)	0.74 (1.21, 0.93)	1.22 (1.45, 0.97)	1.15 (1.44, 0.97)
C <sub>6</sub> H <sub>12</sub> O(7)	0.71 (0.75, 0.90)	0.60 (0.68, 0.93)	0.76 (0.90, 0.86)	0.84 (0.92, 0.90)	1.26 (1.51, 0.69)	1.42 (1.82, 0.76)
C <sub>6</sub> H <sub>14</sub> O(7)	0.73 (0.80, 0.83)	0.69 (0.76, 0.95)	0.84 (0.91, 0.98)	0.71 (0.86, 0.81)	0.56 (0.80, 0.90)	0.67 (0.81, 0.81)
C <sub>8</sub> H <sub>10</sub> O(12)	1.37 (1.60, 0.94)	1.37 (1.59, 0.94)	1.49 (1.69, 0.92)	1.38 (1.62, 0.92)	1.59 (1.94, 0.92)	1.65 (1.93, 0.92)
C <sub>4</sub> H <sub>8</sub> O <sub>2</sub> (9)	1.49 (1.76, 1.00)	1.43 (1.64, 1.00)	1.40 (1.57, 1.00)	1.92 (2.25, 1.00)	1.89 (2.10, 1.00)	2.79 (2.97, 1.00)
C <sub>4</sub> H <sub>10</sub> O <sub>2</sub> (8)	2.68 (2.88, 1.00)	2.60 (2.76, 1.00)	2.30 (2.47, 1.00)	2.84 (3.16, 1.00)	3.48 (3.67, 1.00)	3.65 (3.94, 1.00)
C <sub>5</sub> H <sub>10</sub> O <sub>2</sub> (15)	3.09 (3.45, 0.98)	2.78 (3.14, 0.98)	2.68 (3.05, 0.98)	3.71 (4.13, 0.98)	2.81 (3.24, 0.97)	3.92 (4.49, 0.97)
C <sub>6</sub> H <sub>12</sub> O <sub>2</sub> (16)	2.07 (2.79, 0.95)	2.28 (2.96, 0.95)	2.70 (3.36, 0.95)	1.82 (2.65, 0.95)	3.13 (3.81, 0.94)	2.30 (3.14, 0.94)
C <sub>5</sub> H <sub>12</sub> S(9)	0.61 (0.70, 0.87)	0.64 (0.78, 0.88)	0.45 (0.64, 0.88)	0.67 (0.78, 0.89)	1.05 (1.16, 0.83)	0.74 (0.85, 0.83)
C <sub>6</sub> H <sub>14</sub> S(8)	1.29 (1.83, 0.87)	1.31 (1.85, 0.87)	0.87 (1.57, 0.78)	1.25 (1.79, 0.85)	1.38 (1.70, 0.80)	1.00 (1.48, 0.83)
Total(485)	1.94 (2.75)	2.00 (2.85)	1.87 (2.67)	1.94 (2.75)	2.27 (2.94)	2.63 (3.39)

ular size. This has been exemplified by Tasi *et al.*,<sup>119</sup> for C<sub>1</sub>-C<sub>13</sub> alkanes modelled with G2(MP2,SVP) where large systematic errors were noted when the conventional value of  $\Delta H_f^\circ(0\text{ K})=169.98$  kcal/mol was used for the C atom. The re-evaluated value of 170.11 kcal/mol was shown to reduce systematic errors for that dataset. On the same note, Perdew *et al.*,<sup>120</sup> have remarked on the extensive nature of the self-interaction error in spin-polarized DFAs, and their role in compromising atomization energy predictions.

We have revisited the case of linear alkanes by increasing the set until icosane (C<sub>20</sub>H<sub>42</sub>) and modeling  $\Delta H_f^\circ$  with the four cWFTs along with  $\omega$ B97X-D3 and  $\omega$ B97X-V DFAs. Fig. 12 displays the prediction errors for all 6 methods employing two different values for  $\Delta H_f^\circ(C_{\text{gas}}, 0\text{ K})$ : 169.98 kcal/mol and 170.11 kcal/mol. Barring  $\omega$ B97X-D3 and CBS-QB3, we note deviations to drop systematically when going from the conventional parameter to the one fitted for C<sub>1</sub>-C<sub>13</sub> alkanes in all other methods. We see all cWFTs except CBS-QB3 to benefit

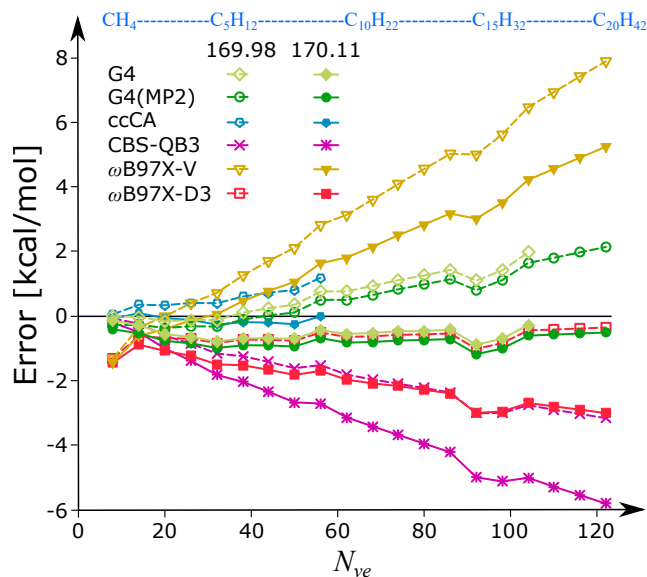
from the systematic shift resulting in reduced prediction errors with ccCA agreeing with the experimental values for C<sub>1</sub>-C<sub>9</sub> alkanes better than G4 and G4(MP2). The DFA  $\omega$ B97X-V showing the maximum error among the methods considered here improves from a mean error of 3.5 kcal/mol to 2.2 kcal/mol. On the other hand,  $\omega$ B97X-D3 which showed excellent agreement with experimental values of  $\Delta H_f^\circ$  with an MUE of 0.7 kcal/mol, when using the conventional  $\Delta H_f^\circ(C_{\text{gas}}, 0\text{ K})$  deteriorates by 1.4 kcal/mol upon using the re-evaluated parameter.

## VII. CONCLUSIONS

A benchmark dataset of experimental  $\Delta H_f^\circ$  for 1694 compounds that are electronically and structurally rich is presented. This dataset was assembled by collecting several previously reported benchmark suites including the ‘legacy’ dataset—G3/05 comprising 247 entries. The resulting set included 102 ‘outliers’ with potentially

TABLE VI. Accuracies of methods in determining the  $\Delta H_f^\circ$  of global minimum of each stoichiometry in ISO32

#	Global minimum (Stoichiometry)	$\Delta H_f^{\circ, \text{exp.}} - \Delta H_f^{\circ, \text{calc.}} (\Delta H_f^{\circ, \text{exp.}} - \Delta H_f^{\circ, \text{calc.}})$						
		G4	G4(MP2)	ccCA	CBS-QB3	$\omega$ B97X-D3	$\omega$ B97X-V	
1	1,3-Butadiene (C <sub>4</sub> H <sub>6</sub> )	26.23	26.52 (-0.29)	25.72 (0.51)	27.21 (-0.98)	28.27 (-2.04)	29.89 (-3.66)	30.25 (-4.02)
2	Cyclopentene (C <sub>5</sub> H <sub>8</sub> )	7.91	8.94 (-1.03)	8.44 (-0.53)	8.92 (-1.01)	10.35 (-2.44)	9.43 (-1.52)	8.03 (-0.12)
3	Cyclopentane (C <sub>5</sub> H <sub>10</sub> )	-18.28	-17.39 (-0.89)	-17.36 (-0.92)	-17.87 (-0.41)	-17.00 (-1.28)	-17.72 (-0.56)	-19.96 (1.68)
4	Methylcyclopentadiene (C <sub>6</sub> H <sub>8</sub> )	23.90	23.68 (0.22)	22.88 (1.02)	24.63 (-0.73)	25.96 (-2.06)	25.33 (-1.43)	24.57 (-0.67)
5	Cyclohexene (C <sub>6</sub> H <sub>10</sub> )	-1.15	-0.66 (-0.49)	-1.14 (-0.01)	-0.38 (-0.77)	1.14 (-2.29)	0.12 (-1.27)	-1.89 (0.74)
6	Cyclohexane (C <sub>6</sub> H <sub>12</sub> )	-29.49	-28.89 (-0.60)	-28.86 (-0.63)	-28.99 (-0.50)	-27.50 (-1.99)	-28.56 (-0.93)	-31.49 (2.00)
7	Toluene (C <sub>7</sub> H <sub>8</sub> )	12.00	11.98 (0.02)	11.02 (0.98)	13.59 (-1.59)	13.60 (-1.60)	13.52 (-1.52)	13.32 (-1.32)
8	Bicyclo[2.2.1]heptane (C <sub>7</sub> H <sub>12</sub> )	-12.96	-13.47 (0.51)	-13.58 (0.62)	-12.87 (-0.09)	-11.91 (-1.05)	-11.73 (-1.23)	-16.44 (3.48)
9	Methylcyclohexane (C <sub>7</sub> H <sub>14</sub> )	-36.98	-36.64 (-0.34)	-36.60 (-0.38)	-36.44 (-0.54)	-34.85 (-2.13)	-35.39 (-1.59)	-38.98 (2.00)
10	Dimethylpentane (C <sub>7</sub> H <sub>16</sub> )	-49.20	-49.27 (0.07)	-49.11 (-0.09)	-49.00 (-0.20)	-47.49 (-1.71)	-45.97 (-3.23)	-49.12 (-0.08)
11	Dimethylbenzene (C <sub>8</sub> H <sub>10</sub> )	4.12	4.05 (0.07)	3.24 (0.88)	6.13 (-2.01)	6.05 (-1.93)	6.05 (-1.93)	5.43 (-1.31)
12	Bicyclo[2.2.2]octane (C <sub>8</sub> H <sub>14</sub> )	-23.66	-22.78 (-0.88)	-22.81 (-0.85)	-21.98 (-1.68)	-20.74 (-2.92)	-20.95 (-2.71)	-26.50 (2.84)
13	(1R,2R,3S)-1,2,3-trimethylcyclopentane (C <sub>8</sub> H <sub>16</sub> )	-45.09	-40.20 (-4.89)	-40.09 (-5.00)	-39.59 (-5.50)	-37.99 (-7.10)	-37.98 (-7.11)	-42.11 (-2.98)
14	Tetramethylbutane (C <sub>8</sub> H <sub>18</sub> )	-53.92	-55.01 (1.09)	-54.92 (1.00)	-53.82 (-0.10)	-52.74 (-1.18)	-48.58 (-5.34)	-53.12 (-0.80)
15	2,3-Dihydro-1H-indene (C <sub>9</sub> H <sub>10</sub> )	14.51	13.90 (0.61)	12.96 (1.55)	16.21 (-1.70)	15.82 (-1.31)	15.18 (-0.67)	13.44 (1.07)
16	1,3,5-Trimethylbenzene (C <sub>9</sub> H <sub>12</sub> )	-3.80	-3.92 (0.12)	-4.58 (0.78)	-1.41 (-2.39)	-1.41 (-2.39)	-1.46 (-2.34)	-2.53 (-1.27)
17	trans-Octahydro-1H-indene (C <sub>9</sub> H <sub>16</sub> )	-31.43	-31.48 (0.05)	-31.51 (0.08)	-30.67 (-0.76)	-29.01 (-2.42)	-30.02 (-1.41)	-35.37 (3.94)
18	(1 $\alpha$ ,3 $\alpha$ ,5 $\alpha$ )-1,3,5-Trimethylcyclohexane (C <sub>9</sub> H <sub>18</sub> )	-50.69	-52.19 (1.50)	-52.10 (1.41)	-51.27 (0.58)	-49.55 (-1.14)	-48.97 (-1.72)	-53.87 (3.18)
19	2-Methylindene (C <sub>10</sub> H <sub>10</sub> )	33.15	28.61 (4.54)	27.31 (5.84)	31.79 (1.36)	31.38 (1.77)	31.17 (1.98)	30.03 (3.12)
20	Adamantane (C <sub>10</sub> H <sub>16</sub> )	-31.90	-33.90 (2.00)	-33.90 (2.00)	-31.58 (-0.32)	-30.87 (-1.03)	-29.63 (-2.27)	-37.88 (5.98)
21	2-Methylaniline (C <sub>7</sub> H <sub>7</sub> N)	12.72	12.37 (0.35)	11.74 (0.98)	13.73 (-1.01)	13.94 (-1.22)	12.62 (0.10)	10.62 (2.10)
22	3-Methyl-2-butanone (C <sub>5</sub> H <sub>10</sub> O)	-62.75	-62.77 (0.02)	-62.32 (-0.43)	-62.53 (-0.22)	-62.55 (-0.20)	-61.63 (-1.12)	-63.78 (1.03)
23	2-Methyl-2-butanol (C <sub>5</sub> H <sub>12</sub> O)	-79.06	-79.32 (0.26)	-78.76 (-0.30)	-79.59 (0.53)	-79.29 (0.23)	-75.95 (-3.11)	-79.12 (0.06)
24	3-3-Dimethyl-2-butanone (C <sub>6</sub> H <sub>12</sub> O)	-69.47	-70.09 (0.62)	-69.63 (0.16)	-69.34 (-0.13)	-69.56 (0.09)	-67.28 (-2.19)	-70.37 (0.90)
25	3-Hexanol (C <sub>6</sub> H <sub>14</sub> O)	-79.30	-80.18 (0.88)	-79.66 (0.36)	-80.85 (1.55)	-79.90 (0.60)	-77.72 (-1.58)	-81.09 (1.79)
26	2,4-Dimethylphenol (C <sub>8</sub> H <sub>10</sub> O)	-38.93	-38.12 (-0.81)	-38.58 (-0.35)	-36.27 (-2.66)	-37.46 (-1.47)	-35.67 (-3.26)	-37.17 (-1.76)
27	2-Methylpropanoic-acid (C <sub>4</sub> H <sub>8</sub> O <sub>2</sub> )	-115.70	-114.12 (-1.58)	-113.46 (-2.24)	-114.35 (-1.35)	-115.21 (-0.49)	-112.70 (-3.00)	-115.28 (-0.42)
28	(2R,3S)-Butane-2,3-diol (C <sub>4</sub> H <sub>10</sub> O <sub>2</sub> )	-114.64	-111.32 (-3.32)	-110.53 (-4.11)	-112.27 (-2.37)	-112.73 (-1.91)	-107.60 (-7.04)	-111.40 (-3.24)
29	3-Methylbutanoic-acid (C <sub>5</sub> H <sub>10</sub> O <sub>2</sub> )	-122.45	-119.99 (-2.46)	-119.37 (-3.08)	-120.26 (-2.19)	-120.79 (-1.66)	-118.53 (-3.92)	-121.57 (-0.88)
30	Hexanoic-acid (C <sub>6</sub> H <sub>12</sub> O <sub>2</sub> )	-122.35	-123.13 (0.78)	-122.48 (0.13)	-123.63 (1.28)	-123.63 (1.28)	-122.35 (0.00)	-125.54 (3.19)
31	2,2-Dimethyl-1-propanethiol (C <sub>5</sub> H <sub>12</sub> S)	-30.83	-31.78 (0.95)	-32.68 (1.85)	-31.90 (1.07)	-31.83 (1.00)	-29.25 (-1.58)	-33.04 (2.21)
32	2-Methyl-2-pentanethiol (C <sub>6</sub> H <sub>14</sub> S)	-35.44	-36.89 (1.45)	-37.60 (2.16)	-36.67 (1.23)	-36.44 (1.00)	-33.51 (-1.93)	-37.93 (2.49)
	MUE		1.05	1.29	1.21	1.65	2.29	1.96

FIG. 12. Systematic errors in G4, G4(MP2), ccCA, CBS-QB3,  $\omega$ B97X-V and  $\omega$ B97X-D3 predictions of  $\Delta H_f^\circ$  due to the choice of  $\Delta H_f^\circ(\text{C}_{\text{gas}}, 0 \text{ K})$  shown for the smallest 20 linear alkanes.

non-negligible experimental uncertainties detected with

a probabilistic approach. The procedure also takes into consideration, uncertainties associated with the reference theory, G4. A more robust approach would be to consider more than one high-fidelity reference methods and make a joint-probabilistic model to prune the dataset. The only tunable parameter in this model is the threshold percentile used for selecting valid benchmarks; this value was set to the 95<sup>th</sup> percentile for the reference method G4. We have adopted a bootstrapping strategy to estimate the variance in the model arising from sampling bias. Our final results are based on the lower bound for the error-threshold to mark an entry as outlier.

For the PPE1694 dataset, we have presented extensive benchmark results of formation enthalpies with 4 cWFTs, *i.e.*, G4, G4(MP2), ccCA and CBS-QB3 as well as with 23 DFAs. Conventional error metrics such as MUE have been reported along with probabilistic metrics such as Q50, Q75, Q90, and Q95, that provide information about the probability and cumulative densities of errors as suggested in other studies<sup>107,121</sup>. When compared to pruned experimental values, among the methods considered in this study, G4 delivers the best performance with an MUE of 1.47 kcal/mol, followed by ccCA and G4(MP2) with MUEs of 1.66 kcal/mol and 1.70 kcal/mol respectively. CBS-QB3 method has

MUE of 1.82 kcal/mol. The semi-empirical methods PM6 and PM7, as expected, result in rather accurate  $\Delta H_f^\circ$  with MUEs  $\approx 4$  kcal/mol. The most popular DFA, B3LYP exhibits a MUE of over 15 kcal/mol. However, its long-range and dispersion corrected versions, namely, CAM-B3LYP and B3LYP-D3 exhibit MUEs  $\approx 4$  kcal/mol, while mGGA method TPSS, the global hybrid functional M06-2X and its D3 corrected variant have MUEs in the 4 – 5 kcal/mol window. Dispersion corrected double hybrid functionals B2PLYP-D3 and mPW2PLYP-D show better performances with overall MUEs in 3 – 4 kcal/mol range. For the prediction of  $\Delta H_f^\circ$ , we found the best performing class of DFAs to be the range-separated method  $\omega$ B97X, and its modifications yielding rather accurate predictions with MUE  $\approx 3$  kcal/mol. As a general trend, we note empirical dispersion corrections to improve prediction accuracy.

Our analyses have revealed that the original G4(MP2) method and the empirical parameterization of the HLC involved in that model retain their transferability going from the G3/05 set with 270 entries to the proposed PPE1694 set that is 6 times larger. This suggests that the prediction accuracy of G4(MP2) to hold not only for closed-shell, organic molecules of the type encountered in the QM9 dataset,<sup>5,30</sup> but also to datasets with free-radicals, non-hydrogens and inorganic hydrides. Interestingly,  $\omega$ B97X-V, with a modest MUE of 2.97 kcal/mol in PPE1694, shows large systematic errors when tested on linear alkanes with 1 – 20 C atoms. This suggests that the parameters that enter into the design of this functional are somewhat overfitted to the training data with small molecules. It will be compelling to see if modern functionals can be designed by benchmarking on the diverse dataset presented here. Similarly, it will be of interest to see if cWFTs based on additional parameterization such as in the G4(MP2)-6X method<sup>122</sup> and its variants<sup>123,124</sup> preserve their transferability going from the small molecules set to the PPE1694 set.

Further, from the entire benchmark suite presented here, we have identified 32 sets of constitutional isomers; reaction enthalpies for this ISO32 dataset were benchmarked over G4, G4(MP2), ccCA, CBS-QB3, and the two best performing DFAs. Isomerization energies are not influenced by HLC parameters, hence they present a stringent test for the prediction capabilities of cWFT methods with empirical corrections. For the prediction of 485 reaction energies, ccCA performs the best with an MUE of 1.86 kcal/mol followed by G4 and G4(MP2) with MUEs 1.94 kcal/mol and 2.00 kcal/mol respectively. In this case, the DFAs  $\omega$ B97-XD3 and  $\omega$ B97-XV have also yielded excellent predictions with MUEs of  $\approx 2$ -2.5. When extending the application of G4(MP2) method to molecules with large number of C atoms, we find the prediction accuracy to be sensitive to an empirical atomic parameter, which suggests that a careful evaluation of these parameters for all atom types is essential to prevent systematic accumulation of errors.

Such calibration should be done with a method such as W4 or HEAT-456(Q) that is more robust than the method considered here. Preferably such an effort could be undertaken by pruning the total dataset and retaining only highly-precise experimental entries. Thermochemistry modeling done at such a rigour has been shown to be sensitive even to the effect anharmonicity has on molecular ZPVE<sup>125,126</sup>, hence these effects must be incorporated with methods such as second-order vibrational perturbation theory (VPT2)<sup>127,128</sup> that are amenable for large scale modeling.

## VIII. ACKNOWLEDGEMENTS

SKD is grateful to TIFR Hyderabad for a junior research fellowship. All authors thank TIFR for support. This project was funded by intramural funds at TIFR Hyderabad from the Department of Atomic Energy (DAE). All calculations have been performed using the Helios computer cluster, which is an integral part of the MolDis Big Data facility, TIFR Hyderabad (<https://moldis.tifrh.res.in/>).

## IX. DATA AVAILABILITY

The data that supports the findings of this study are available within the article and its supplementary material.

## APPENDIX: EMPIRICAL THERMOCHEMISTRY PARAMETERS

## X. REFERENCES

- <sup>1</sup>J. Cioslowski, *Quantum-mechanical prediction of thermochemical data* (Springer Science & Business Media, 2002).
- <sup>2</sup>K. K. Irikura and D. J. Frurip, *Computational Thermochemistry* (ACS Publications, 1998) Chap. 1, pp. 2-18.
- <sup>3</sup>O. A. von Lilienfeld, *Angew. Chem. Int. Ed.* **57**, 4164 (2018).
- <sup>4</sup>R. Ramakrishnan and O. A. von Lilienfeld, *Rev. Comp. Ch.* **30**, 225 (2017).
- <sup>5</sup>B. Narayanan, P. C. Redfern, R. S. Assary, and L. A. Curtiss, *Chem. Sci.* **10**, 7449 (2019).
- <sup>6</sup>J. Hachmann, R. Olivares-Amaya, S. Atahan-Evrenk, C. Amador-Bedolla, R. S. Sánchez-Carrera, A. Gold-Parker, L. Vogt, A. M. Brockway, and A. Aspuru-Guzik, *J. Phys. Chem. Lett.* **2**, 2241 (2011).
- <sup>7</sup>S. Chakraborty, P. Kayastha, and R. Ramakrishnan, *J. Chem. Phys.* **150**, 114106 (2019).
- <sup>8</sup>J. Arús-Pous, M. Awale, D. Probst, and J.-L. Reymond, *CHIMIA* **73**, 1018 (2019).
- <sup>9</sup>J. Aston, *Ind. Eng. Chem.* **34**, 514 (1942).
- <sup>10</sup>H. Duus, *Ind. Eng. Chem.* **47**, 1445 (1955).
- <sup>11</sup>A. S. Rodgers, *J. Phys. Chem.* **71**, 1996 (1967).
- <sup>12</sup>O. V. Dorofeeva, V. P. Novikov, and D. B. Neumann, *J. Phys. Chem. Ref. Data* **30**, 475 (2001).
- <sup>13</sup>L. A. Curtiss, P. C. Redfern, and D. J. Frurip, in *Reviews of Computational Chemistry*, Vol. 15, edited by K. B. Lipkowitz and D. B. Boyd (Wiley VCH, New York, 2000) pp. 147-211.

TABLE VII. Heats of formation of atoms at 0 K,  $\Delta H_f^\circ(0\text{ K})$ , and enthalpy corrections, for elements in their standard states,  $H^\circ(298\text{ K}) - H^\circ(0\text{ K})$ . Unless specified, all values are taken from Ref. 129. For elements for which more than one value are available, we have utilized the more recent one marked by bold font. All values are in kcal/mol.

Atom	$\Delta H_f^\circ(0\text{ K})$	$H^\circ(298\text{ K}) - H^\circ(0\text{ K})$
H	51.63	1.01
Li	37.69	1.10
Be	76.48	0.46
B	136.2	0.29
C	169.98	0.25
N	112.53	1.04
O	58.99	1.04
F	18.47	1.05
Na	25.69	1.54
Mg	34.87	1.19
Al	78.23	1.08
Si	106.6	0.76
P	75.42	1.28
S	65.66	1.05
Cl	28.59	1.10
K	21.4830 <sup>130</sup>	1.6926 <sup>130</sup>
Ca	42.3850 <sup>130</sup>	1.3709 <sup>130</sup>
Ga	64.7633 <sup>130</sup>	1.3291 <sup>130</sup>
Br	28.1836 <sup>131</sup>	2.930 <sup>131,132</sup>
Ge	<b>89.354</b> <sup>133</sup> , 88.2 <sup>134</sup>	1.104 <sup>133,135</sup>
As	<b>68.86</b> <sup>136</sup> , 68.8 <sup>133,137</sup>	1.23 <sup>135</sup>
Se	57.899 <sup>138</sup>	1.319 <sup>138</sup>

- <sup>14</sup>L. A. Curtiss, P. C. Redfern, and K. Raghavachari, *WIREs Comput. Mol. Sci.* **1**, 810 (2011).
- <sup>15</sup>F. Jensen, *Introduction to computational chemistry* (John Wiley & sons, 2017).
- <sup>16</sup>A. Karton, *WIREs Comput. Mol. Sci.* **6**, 292 (2016).
- <sup>17</sup>A. Karton, E. Rabinovich, J. M. Martin, and B. Ruscic, *J. Chem. Phys.* **125**, 144108 (2006).
- <sup>18</sup>Y. J. Bomble, J. Vázquez, M. Kállay, C. Michauk, P. G. Szalay, A. G. Császár, J. Gauss, and J. F. Stanton, *J. Chem. Phys.* **125**, 064108 (2006).
- <sup>19</sup>M. E. Harding, J. Vázquez, B. Ruscic, A. K. Wilson, J. Gauss, and J. F. Stanton, *J. Chem. Phys.* **128**, 114111 (2008).
- <sup>20</sup>D. W. Rogers, *Heats of hydrogenation: experimental and computational hydrogen thermochemistry of organic compounds* (World Scientific: Long Island, NY, 2006).
- <sup>21</sup>J. M. Martin, *Annu. Rep. Comput. Chem.* **1**, 31 (2005).
- <sup>22</sup>J. Montgomery Jr, J. Ochterski, and G. Petersson, *J. Chem. Phys.* **101**, 5900 (1994).
- <sup>23</sup>L. A. Curtiss, P. C. Redfern, and K. Raghavachari, *J. Chem. Phys.* **126**, 084108 (2007).
- <sup>24</sup>N. J. DeYonker, T. R. Cundari, and A. K. Wilson, *J. Chem. Phys.* **124**, 114104 (2006).
- <sup>25</sup>N. J. DeYonker, T. Grimes, S. Yockel, A. Dinescu, B. Mintz, T. R. Cundari, and A. K. Wilson, *J. Chem. Phys.* **125**, 104111 (2006).
- <sup>26</sup>A. K. Wilson, N. J. DeYonker, and T. R. Cundari, in *Advances in the Theory of Atomic and Molecular Systems (Progress in Theoretical Chemistry and Physics)*, Vol. 19, edited by P. Piecuch, J. Maruani, G. Delgado-Barrio, and S. Wison (Springer, Netherlands, 2009) pp. 197–224.
- <sup>27</sup>L. Ruddigkeit, R. Van Deursen, L. C. Blum, and J.-L. Reymond, *J. Chem. Inf. Model.* **52**, 2864 (2012).
- <sup>28</sup>F. A. Faber, A. S. Christensen, B. Huang, and O. A. von Lilienfeld, *J. Chem. Phys.* **148**, 241717 (2018).

- <sup>29</sup>N. Lubbers, J. S. Smith, and K. Barros, *J. Chem. Phys.* **148**, 241715 (2018).
- <sup>30</sup>R. Ramakrishnan, P. O. Dral, M. Rupp, and O. A. von Lilienfeld, *Scientific Data* **1**, 140022 (2014).
- <sup>31</sup>R. Ramakrishnan, P. O. Dral, M. Rupp, and O. A. von Lilienfeld, *J. Chem. Theory Comput.* **11**, 2087 (2015).
- <sup>32</sup>H. Kim, J. Y. Park, and S. Choi, *Scientific Data* **6**, 109 (2019).
- <sup>33</sup>L. Ward, B. Blaiszik, I. Foster, R. S. Assary, B. Narayanan, and L. Curtiss, *MRS Commun.* **9**, 891 (2019).
- <sup>34</sup>N. K. Dandu, L. Ward, R. S. Assary, P. C. Redfern, B. Narayanan, I. T. Foster, and L. A. Curtiss, *J. Phys. Chem. A* (2020), 10.1021/acs.jpca.0c01777.
- <sup>35</sup>J. Pedley, R. D. Naylor, S. P. Kirby, *et al.*, *Thermochemical data of organic compounds* (Chapman and Hall, 1986).
- <sup>36</sup>J. Pedley, *Thermochemical data and structures of organic compounds*, Vol. 1 (CRC Press, 1994).
- <sup>37</sup>L. A. Curtiss, P. C. Redfern, and K. Raghavachari, *J. Chem. Phys.* **127**, 124105 (2007).
- <sup>38</sup>N. J. DeYonker, B. R. Wilson, A. W. Pierpont, T. R. Cundari, and A. K. Wilson, *Mol. Phys.* **107**, 1107 (2009).
- <sup>39</sup>L. A. Curtiss, P. C. Redfern, and K. Raghavachari, *J. Chem. Phys.* **123**, 124107 (2005).
- <sup>40</sup>M. Schwilk, D. N. Tahchieva, and O. A. von Lilienfeld, arXiv preprint arXiv:2004.10600 (2020).
- <sup>41</sup>F. Neese, *WIREs Comput. Mol. Sci.* **2**, 73 (2012).
- <sup>42</sup>F. Neese, *WIREs Comput. Mol. Sci.* **8**, e1327 (2018).
- <sup>43</sup>M. J. Frisch, G. W. Trucks, H. B. Schlegel, G. E. Scuseria, M. A. Robb, J. R. Cheeseman, G. Scalmani, V. Barone, G. A. Petersson, H. Nakatsuji, X. Li, M. Caricato, A. V. Marenich, J. Bloino, B. G. Janesko, R. Gomperts, B. Mennucci, H. P. Hratchian, J. V. Ortiz, A. F. Izmaylov, J. L. Sonnenberg, D. Williams-Young, F. Ding, F. Lipparini, F. Egidi, J. Goings, B. Peng, A. Petrone, T. Henderson, D. Ranasinghe, V. G. Zakrzewski, J. Gao, N. Rega, G. Zheng, W. Liang, M. Hada, M. Ehara, K. Toyota, R. Fukuda, J. Hasegawa, M. Ishida, T. Nakajima, Y. Honda, O. Kitao, H. Nakai, T. Vreven, K. Throssell, J. A. Montgomery, Jr., J. E. Peralta, F. Ogliaro, M. J. Bearpark, J. J. Heyd, E. N. Brothers, K. N. Kudin, V. N. Staroverov, T. A. Keith, R. Kobayashi, J. Normand, K. Raghavachari, A. P. Rendell, J. C. Burant, S. S. Iyengar, J. Tomasi, M. Cossi, J. M. Millam, M. Klene, C. Adamo, R. Cammi, J. W. Ochterski, R. L. Martin, K. Morokuma, O. Farkas, J. B. Foresman, and D. J. Fox, "Gaussian 16 Revision C.01," (2016), gaussian Inc. Wallingford CT.
- <sup>44</sup>J. J. Stewart, *J. Mol. Model.* **13**, 1173 (2007).
- <sup>45</sup>J. J. Stewart, *J. Mol. Model.* **19**, 1 (2013).
- <sup>46</sup>J. J. Stewart, "Mopac2016," (2016), Stewart Computational Chemistry, Colorado Springs, CO, USA, Available at <http://OpenMOPAC.net>.
- <sup>47</sup>J. P. Perdew and K. Schmidt, in *AIP Conference Proceedings*, Vol. 577 (American Institute of Physics, 2001) pp. 1–20.
- <sup>48</sup>A. D. Becke, *Phys. Rev. A* **38**, 3098 (1988).
- <sup>49</sup>J. Perdew, J. Chevary, and S. Vosko, *Phys. Rev. B* **46**, 6671 (1992).
- <sup>50</sup>J. P. Perdew, K. Burke, and M. Ernzerhof, *Phys. Rev. Lett.* **78**, 1396 (1997).
- <sup>51</sup>A. D. Becke, *J. Chem. Phys.* **98**, 5648 (1993).
- <sup>52</sup>A. J. Cohen and N. C. Handy, *Mol. Phys.* **99**, 607 (2001).
- <sup>53</sup>X. Xu and W. A. Goddard, *Proc. Natl. Acad. Sci. USA* **101**, 2673 (2004).
- <sup>54</sup>C. Adamo and V. Barone, *J. Chem. Phys.* **110**, 6158 (1999).
- <sup>55</sup>J. Tao, J. P. Perdew, V. N. Staroverov, and G. E. Scuseria, *Phys. Rev. Lett.* **91**, 146401 (2003).
- <sup>56</sup>S. Grimme, *J. Phys. Chem. A* **109**, 3067 (2005).
- <sup>57</sup>Y. Zhao and D. G. Truhlar, *Theor. Chem. Acc.* **120**, 215 (2008).
- <sup>58</sup>T. Yanai, D. P. Tew, and N. C. Handy, *Chem. Phys. Lett.* **393**, 51 (2004).
- <sup>59</sup>J.-D. Chai and M. Head-Gordon, *Phys. Chem. Chem. Phys.* **10**, 6615 (2008).
- <sup>60</sup>N. Mardirossian and M. Head-Gordon, *Phys. Chem. Chem. Phys.* **16**, 9904 (2014).
- <sup>61</sup>N. Mardirossian and M. Head-Gordon, *J. Chem. Phys.* **144**, 214110 (2016).

- <sup>62</sup>S. Grimme, S. Ehrlich, and L. Goerigk, *J. Comp. Chem.* **32**, 1456 (2011).
- <sup>63</sup>A. D. Becke and E. R. Johnson, *J. Chem. Phys.* **123**, 154101 (2005).
- <sup>64</sup>E. R. Johnson and A. D. Becke, *J. Chem. Phys.* **123**, 024101 (2005).
- <sup>65</sup>E. R. Johnson and A. D. Becke, *J. Chem. Phys.* **124**, 174104 (2006).
- <sup>66</sup>S. Grimme, *J. Chem. Phys.* **124**, 034108 (2006).
- <sup>67</sup>S. Grimme, J. Antony, S. Ehrlich, and H. Krieg, *J. Chem. Phys.* **132**, 154104 (2010).
- <sup>68</sup>T. Schwabe and S. Grimme, *Phys. Chem. Chem. Phys.* **9**, 3397 (2007).
- <sup>69</sup>P. Linstrom and E. W.G. Mallard, "NIST chemistry webbook, NIST Standard Reference Database Number 69, National Institute of Standards and Technology, Gaithersburg MD, 20899," (2020), (Accessed December 2019).
- <sup>70</sup>H. E. Pence and A. Williams, "Chemspider: An online chemical information resource," (2010), (Accessed December 2019).
- <sup>71</sup>S. Kim, J. Chen, T. Cheng, A. Gindulyte, J. He, S. He, Q. Li, B. A. Shoemaker, P. A. Thiessen, B. Yu, *et al.*, *Nucleic Acids Res.* **47**, D1102 (2019).
- <sup>72</sup>M. D. Hanwell, D. E. Curtis, D. C. Lonie, T. Vandermeersch, E. Zurek, and G. R. Hutchison, *J. Cheminform* **4**, 17 (2012).
- <sup>73</sup>A. K. Rappé, C. J. Casewit, K. Colwell, W. A. Goddard III, and W. M. Skiff, *J. Am. Chem. Soc.* **114**, 10024 (1992).
- <sup>74</sup>F. Weigend and R. Ahlrichs, *Phys. Chem. Chem. Phys.* **7**, 3297 (2005).
- <sup>75</sup>J. W. Ochterski, *Thermochemistry in gaussian*, [www.gaussian.com](http://www.gaussian.com) (2000), Accessed December 2019.
- <sup>76</sup>Note that in Table I of Ref. 78  $\text{SeH}^+$  has to be  $\text{SeH}$ .
- <sup>77</sup>L. A. Curtiss, M. P. McGrath, J.-P. Blaudeau, N. E. Davis, R. C. Binning Jr, and L. Radom, *J. Chem. Phys.* **103**, 6104 (1995).
- <sup>78</sup>L. A. Curtiss, P. C. Redfern, V. Rassolov, G. Kedziora, and J. A. Pople, *J. Chem. Phys.* **114**, 9287 (2001).
- <sup>79</sup>N. L. Allinger, J. T. Fermann, W. D. Allen, and H. F. Schaefer III, *J. Chem. Phys.* **106**, 5143 (1997).
- <sup>80</sup>L. A. Curtiss, K. Raghavachari, P. C. Redfern, V. Rassolov, and J. A. Pople, *J. Chem. Phys.* **109**, 7764 (1998).
- <sup>81</sup>J. M. Martin, *Theor. Chem. Acc.* **97**, 227 (1997).
- <sup>82</sup>J. M. Martin, *Chem. Phys. Lett.* **259**, 669 (1996).
- <sup>83</sup>J. Martin, *J. Chem. Phys.* **97**, 5012 (1992).
- <sup>84</sup>J. M. Martin, *J. Chem. Phys.* **100**, 8186 (1994).
- <sup>85</sup>J. A. Pople, M. Head-Gordon, D. J. Fox, K. Raghavachari, and L. A. Curtiss, *J. Chem. Phys.* **90**, 5622 (1989).
- <sup>86</sup>L. A. Curtiss, K. Raghavachari, G. W. Trucks, and J. A. Pople, *J. Chem. Phys.* **94**, 7221 (1991).
- <sup>87</sup>N. J. DeYonker, T. G. Williams, A. E. Imel, T. R. Cundari, and A. K. Wilson, *J. Chem. Phys.* **131**, 024106 (2009).
- <sup>88</sup>M. L. Laury, N. J. DeYonker, W. Jiang, and A. K. Wilson, *J. Chem. Phys.* **135**, 214103 (2011).
- <sup>89</sup>C. Peterson, D. Penchoff, and A. Wilson, in *Annual Reports in Computational Chemistry*, Vol. 12 (Elsevier, 2016) pp. 3–45.
- <sup>90</sup>B. A. Hess, *Phys. Rev. A* **32**, 756 (1985).
- <sup>91</sup>B. A. Hess, *Phys. Rev. A* **33**, 3742 (1986).
- <sup>92</sup>G. Jansen and B. A. Hess, *Phys. Rev. A* **39**, 6016 (1989).
- <sup>93</sup>M. Reiher, *WIREs Comput. Mol. Sci.* **2**, 139 (2012).
- <sup>94</sup>N. J. DeYonker, K. A. Peterson, G. Steyl, A. K. Wilson, and T. R. Cundari, *J. Phys. Chem. A* **111**, 11269 (2007).
- <sup>95</sup>T. H. Dunning Jr, K. A. Peterson, and A. K. Wilson, *J. Chem. Phys.* **114**, 9244 (2001).
- <sup>96</sup>N. J. DeYonker, B. Mintz, T. R. Cundari, and A. K. Wilson, *J. Chem. Theory Comput.* **4**, 328 (2008).
- <sup>97</sup>M. M. Ghahremanpour, P. J. Van Maaren, and D. Van Der Spoel, *Scientific Data* **5**, 180062 (2018).
- <sup>98</sup>P. R. Schreiner, A. A. Fokin, R. A. Pascal, and A. de Meijere, *Org. Lett.* **8**, 3635 (2006).
- <sup>99</sup>A. Sengupta and K. Raghavachari, *J. Chem. Theory Comput.* **10**, 4342 (2014).
- <sup>100</sup>O. V. Dorofeeva and M. A. Filimonova, *J. Chem. Thermodyn.* **126**, 31 (2018).
- <sup>101</sup>E. Paulechka and A. Kazakov, *J. Phys. Chem. A* **121**, 4379 (2017).
- <sup>102</sup>B. Ruscic, *Int. J. Quantum Chem.* **114**, 1097 (2014).
- <sup>103</sup>G. N. Simm, J. Proppe, and M. Reiher, *CHIMIA* **71**, 202 (2017).
- <sup>104</sup>P. Pernot and A. Savin, *J. Chem. Phys.* **148**, 241707 (2018).
- <sup>105</sup>A. J. Thakkar and T. Wu, *J. Chem. Phys.* **143**, 144302 (2015).
- <sup>106</sup>T. Wu, Y. N. Kalugina, and A. J. Thakkar, *Chem. Phys. Lett.* **635**, 257 (2015).
- <sup>107</sup>P. Pernot and A. Savin, *J. Chem. Phys.* **152**, 164108 (2020).
- <sup>108</sup>A. Savin and E. R. Johnson, "Judging density-functional approximations: Some pitfalls of statistics," in *Density Functionals: Thermochemistry*, edited by E. R. Johnson (Springer International Publishing, Cham, 2015) pp. 81–95.
- <sup>109</sup>J. P. Perdew, J. Sun, A. J. Garza, and G. E. Scuseria, *Z. Phys. Chem.* **230**, 737 (2016).
- <sup>110</sup>A. Gramacki, *Nonparametric kernel density estimation and its computational aspects* (Springer, 2018).
- <sup>111</sup>M. Jaidann, S. Roy, H. Abou-Rachid, and L.-S. Lussier, *J. Hazard. Mater.* **176**, 165 (2010).
- <sup>112</sup>L. Türker, S. Gümüş, and T. Atalar, *J. Energ. Mater.* **28**, 139 (2010).
- <sup>113</sup>J. P. Guthrie, *J. Phys. Chem. A* **105**, 9196 (2001).
- <sup>114</sup>C. Spearman, *Am. J. Psychol.* **15**, 72 (1904), Reprinted: *Int. J. Epidemiol* 2010;39:1137–50.
- <sup>115</sup>S. Grimme, M. Steinmetz, and M. Korth, *J. Org. Chem.* **72**, 2118 (2007).
- <sup>116</sup>S. Luo, Y. Zhao, and D. G. Truhlar, *Phys. Chem. Chem. Phys.* **13**, 13683 (2011).
- <sup>117</sup>K. W. Sattelmeyer, J. Tirado-Rives, and W. L. Jorgensen, *J. Phys. Chem. A* **110**, 13551 (2006).
- <sup>118</sup>A. Karton and J. M. Martin, *Mol. Phys.* **110**, 2477 (2012).
- <sup>119</sup>G. Tasi, R. Izsák, G. Matisz, A. G. Császár, M. Kállay, B. Ruscic, and J. F. Stanton, *ChemPhysChem* **7**, 1664 (2006).
- <sup>120</sup>J. P. Perdew, J. Sun, A. Ruzsinszky, P. D. Mezei, and G. I. Csonka, *Period. Polytech. Chem. Eng.* **60**, 2 (2016).
- <sup>121</sup>P. Pernot, B. Huang, and A. Savin, *Mach. Learn.: Sci. Technol.* **4**, 1, 035011 (2020).
- <sup>122</sup>B. Chan, J. Deng, and L. Radom, *J. Chem. Theory Comput.* **7**, 112 (2010).
- <sup>123</sup>B. Chan, A. Karton, and K. Raghavachari, *J. Chem. Theory Comput.* **15**, 4478 (2019).
- <sup>124</sup>E. Semidalas and J. M. Martin, *J. Chem. Theory Comput.* (2020), 10.1021/acs.jctc.0c00189.
- <sup>125</sup>F. Pfeiffer, G. Rauhut, D. Feller, and K. A. Peterson, *J. Chem. Phys.* **138**, 044311 (2013).
- <sup>126</sup>K. A. Peterson, D. Feller, and D. A. Dixon, *Theor. Chem. Acc.* **131**, 1079 (2012).
- <sup>127</sup>V. Barone, *J. Chem. Phys.* **122**, 014108 (2005).
- <sup>128</sup>R. Ramakrishnan and G. Rauhut, *J. Chem. Phys.* **142**, 154118 (2015).
- <sup>129</sup>L. A. Curtiss, K. Raghavachari, P. C. Redfern, and J. A. Pople, *J. Chem. Phys.* **106**, 1063 (1997).
- <sup>130</sup>M. Chase, C. Davies, J. Downey, D. Frurip, R. McDonald, and A. Syverud, "NIST-JANAF Thermochemical Tables (ver. 1.0), online, standard reference data program; national institute of standards and technology: Gaithersburg, md, usa, 1985," .
- <sup>131</sup>D. Trogolo and J. S. Arey, *Phys. Chem. Chem. Phys.* **17**, 3584 (2015).
- <sup>132</sup>J. Cox, D. D. Wagman, and V. A. Medvedev, *CODATA key values for thermodynamics* (Chem/Mats-Sci/E, 1989).
- <sup>133</sup>P. M. Mayer, J.-F. Gal, and L. Radom, *Int. J. Mass Spectrom. Ion Processes* **167**, 689 (1997).
- <sup>134</sup>B. Ruscic, M. Schwarz, and J. Berkowitz, *J. Chem. Phys.* **92**, 1865 (1990).
- <sup>135</sup>D. Wagman, W. Evans, V. Parker, and R. Schumm, *J. Phys. Chem. Ref. Data* **11** (1982).
- <sup>136</sup>D. Feller, M. Vasiliu, D. J. Grant, and D. A. Dixon, *J. Phys. Chem. A* **115**, 14667 (2011).
- <sup>137</sup>R. Binning Jr and L. A. Curtiss, *J. Chem. Phys.* **92**, 1860 (1990).
- <sup>138</sup>L. Wang, *Int. J. Mass Spectrom.* **264**, 84 (2007).